NASA TECHNICAL REPORT

NASA TR R-317

NASA TR R-317

A NUMERICAL ANALYSIS OF THE USE OF PERFORATED WALLS TO CONTROL SHOCK LOCATION AND MOVEMENT IN AN INTERNAL-COMPRESSION SUPERSONIC INLET

by Clarence W. Matthews

Langley Research Center
Langley Station, Hampton, Va.

NATIONAL AERONAUTICS AND SPACE ADMINISTRATION • WASHINGTON, D. C. • JULY 1969

1. Report No. NASA TR R-317	2. Government Accession No.	3. Recipient's Catalog No.
4. Title and Subtitle A NUMERICAL ANALYSIS OF THE USE OF PERFORATED WALLS TO CONTROL SHOCK LOCATION AND MOVEMENT IN AN INTERNAL-COMPRESSION SUPERSONIC INLET		5. Report Date July 1969 6. Performing Organization Code
7. Author(s) Clarence W. Matthews		8. Performing Organization Report No. L-6342
9. Performing Organization Name and Address NASA Langley Research Center, Langley Station, Hampton, Va. 23365		10. Work Unit No. 720-03-00-02-23 11. Contract or Grant No.
12. Sponsoring Agency Name and Address National Aeronautics and Space Administration, Washington, D.C. 20546		13. Type of Report and Period Covered Technical Report 14. Sponsoring Agency Code

15. Supplementary Notes

16. Abstract

This paper presents an analysis of the ability of a perforated wall in an internal-compression supersonic inlet to control the motion of the shock due to a variety of transients in the flow values at the engine face. The method of one-dimensional unsteady-flow characteristics was used to calculate the shock motion. The perforated walls were found to contain the shock within the inlet for appreciably larger transient magnitudes than was possible with solid walls.

17. Key Words Suggested by Author(s) Dynamic properties of inlets Shock motion in inlets Internal-compression supersonic inlets Perforated supersonic-inlet walls Unsteady flow characteristics	18. Distribution Statement Unclassified – Unlimited		
19. Security Classif. (of this report) Unclassified	20. Security Classif. (of this page) Unclassified	21. No. of Pages 52	22. Price* $3.00

*For sale by the Clearinghouse for Federal Scientific and Technical Information
Springfield, Virginia 22151

A NUMERICAL ANALYSIS OF THE USE OF PERFORATED WALLS TO CONTROL SHOCK LOCATION AND MOVEMENT IN AN INTERNAL-COMPRESSION SUPERSONIC INLET

By Clarence W. Matthews
Langley Research Center

SUMMARY

This paper presents an analysis of the shock motions in an internal-compression supersonic inlet with the walls in the supersonic section so designed that they are perforated to subsonic flow and solid to supersonic flow. The shock motion is computed with a computer program utilizing one-dimensional unsteady-flow characteristic theory. The perforated walls were studied to determine their ability to control the shock motion, and especially to contain the shock within the inlet for the application of various flow transients to the engine face.

It was found that the perforated walls controlled the shock motion, thereby containing the shock within the inlet for much larger transient magnitudes than was possible with solid walls. The response of the shock motion to the engine-face transients indicated that the response characteristics for short impulse-type transients were sufficiently linear to allow the use of a transfer function over a limited range. However, period differences and the development of a limit cycle in the shock motion when the shock position is ahead of the throat seriously restrict or even prevent the use of transfer functions to express the shock motion for long periods or throttle-chop transients.

INTRODUCTION

Supersonic inlets which incorporate large amounts of internal contraction operate most efficiently if the normal shock is maintained at the throat. However, if the shock moves upstream of the throat, the flow in the entire inlet breaks down. Hence, control of the normal-shock system to prevent breakdown of the flow in the inlet is imperative if the inlet is to operate efficiently. Various methods of controlling this shock motion have been studied experimentally, such as the use of pressure sensors or probes or the use of subsonic Mach numbers to vary either the bypass flow or the local area distribution of the inlet (refs. 1 to 5). Another method of control which avoids elaborate mechanisms is the use of aerodynamically variable or "educated" holes in the walls of the converging

supersonic portion of the inlet which bleed much of the flow in the subsonic portion behind the shock but bleed little of the supersonic flow ahead of the shock (refs. 6 and 7). An advantage of this method is that it acts as fast as the shock motion itself and so has the potentiality of preventing possible unstarts of the inlet in case severe engine transients occur. Also, after such a transient ceases and operation returns to normal, the "perforated" wall has the potentiality of quickly returning the inlet flow to its normal operating condition.

This type of inlet was studied in some detail in the experiments of reference 7, which gives pressure recovery results, ability to restart, and in several cases the ability to hold the shock stable in the contracting portion of the diffuser. It does not, however, present much information on the actual shock motion due to various engine transients or on the increase in the amplitude of such transients that the wall is capable of controlling.

It is the purpose of this paper to present a study of the use of perforated walls in an internal-compression inlet to control the motion of the normal shock due to the application of various transient flow-property changes at the engine face. The analysis considers various degrees of wall perforation up to 40 percent open, as well as transient changes in velocity, pressure, and mass flow of as much as 50 to 60 percent at the engine face. Some discussion of the computer program used to compile the unsteady flow field is included.

SYMBOLS

A	local cross-sectional area of inlet, meters
A_{ch}	restricted area at engine face such that flow is choked
a	nondimensional sonic speed (nondimensionalized with respect to sonic speed at initial free-stream conditions)
c	speed of sound, meters/sec
d	diameter of area equivalent to cross section of inlet, meters
F	body force, newtons
f	entropy function, $\frac{DS}{D\tau} = f(a,u,S,\xi,\tau)$
h	height of entrance to inlet, meters

k coefficient having the sign of the transient disturbance and proportional to its magnitude

M Mach number

m_e mass flow rate at engine face nondimensionalized with respect to mass flow rate at entrance of inlet

m_w mass flow rate per unit length of perforated upper wall of inlet, kilograms/meter-second

$P = \sigma a + u$

p static pressure, newtons/meter^2

p_e static pressure at engine face nondimensionalized with respect to free-stream total pressure

$Q = \sigma a - u$

S nondimensional value of entropy, $\dfrac{\text{Specific entropy}}{(\gamma - 1)(\text{Specific heat at constant pressure})}$

u nondimensional local velocity (nondimensionalized with respect to sonic speed at initial free-stream conditions)

u_e value of u at engine face

W nondimensional shock velocity (nondimensionalized with respect to sonic speed at initial free-stream conditions)

w width of inlet, meters

x length coordinate along inlet axis, meters

γ ratio of specific heats

$\dfrac{\delta_+}{\delta\tau}$ line derivative along P-line (a line of slope $u + a$), $\dfrac{\partial}{\partial\tau} + (u + a)\dfrac{\partial}{\partial\xi}$

$\dfrac{\delta_-}{\delta\tau}$ line derivative along Q-line (a line of slope $u - a$), $\dfrac{\partial}{\partial\tau} + (u - a)\dfrac{\partial}{\partial\xi}$

$\frac{DS}{D\tau}$ nondimensional substantial derivative of entropy, that is, derivative along a streamline, $\frac{\partial S}{\partial \tau} + u \frac{\partial S}{\partial \xi}$

$\xi = \frac{x}{h}$

ρ density of fluid, kilograms/meter^3

$\sigma = \frac{2}{\gamma - 1}$

τ nondimensional time; unit value of τ equals h/c

Ψ nondimensional value of mass removed per unit length in unit time, $hc_\infty m_w / \gamma A p_\infty$

ψ local proportion of open area to total area of walls

ω angular frequency of sine or cosine transients

Subscripts:

f in front of shock

h value of flow property in wall perforation

r at rear of shock

s at shock

∞ free-stream condition

THEORY

Perforated Walls for Control of Shock Motion

Control of the shock motion in an internal-compression supersonic inlet is necessary because serious losses in mass flow, pressure recovery, and drag effects occur if the shock is expelled from the inlet. It is well known that such shock expulsion does occur whenever the shock is forced ahead of the throat of the inlet by either engine-face or inlet-entrance transients in the flow. This expulsion occurs primarily because the shock position is unstable in a region wherein the derivative of the area with respect to

distance along the inlet is negative. A possible means of preventing this expulsion is to reduce the pressure behind the shock, thereby drawing the shock back to its stable region downstream of the throat. This result may be accomplished by bleeding the air from the inlet through perforations in the wall.

References 6 and 7 present results of studies of the behavior of inlets with perforated walls. These studies, which were mostly experimental, indicate that the shock will remain within the inlet whenever a transient such as a throttle chop is applied to the inlet. However, because of experimental limitations, no detailed study of the actual shock motion caused by various transients has been made. Such an analysis would be difficult to make experimentally, but can be accomplished by computation with a one-dimensional time-variant characteristic system. Although several of the studies used an inlet with "educated" holes which bled much of the subsonic flow but little of the supersonic exit flow, the present analysis considers an inlet which has spring-loaded flap doors over the surface of the inlet. (See figs. 1(a) and 1(b).) These doors are considered to have sufficient spring loading to close them when the low-pressure supersonic flow covers the doors and to open them when the high-pressure subsonic flow covers the doors. Although the physical realization of such a door might present many problems, such as unstable flapping or removal of the fluid which escapes through the walls, the condition is simply expressed analytically by setting ψ, the proportion of open area in the wall, equal to zero if the flow is supersonic and equal to some given value if the flow is subsonic. It is assumed that the pressure exterior to the inlet is small enough to allow any flow through an opening to be sonic, and that the holes are completely filled with flow.

Computing Program

The program used to compute the shock motion in an inlet due to various disturbances involves an integration over a ξ,τ field, where ξ is the nondimensional distance along the axis of the inlet and τ is the nondimensional time, of the one-dimensional unsteady-flow characteristic equations presented in reference 8. These equations are expressed in terms of the sonic speed a, the flow velocity u, and the entropy S. The values u and a are nondimensionalized with respect to the speed of sound at free-stream conditions, that is, $a = 1$ at initial free-stream conditions. The unit distance for ξ is considered to be the height of the two-dimensional inlet at the inlet entrance. The corresponding unit value of τ is the time for a free-stream sound wave to traverse the unit distance for ξ. The characteristic equations actually express the changes in P and Q, functions of u and a, along the two characteristic directions $\frac{d\xi}{d\tau} = u + a$ and $\frac{d\xi}{d\tau} = u - a$, and the change in S along the streamline $\frac{d\xi}{d\tau} = u$.

Flow Equations

Equations for characteristic phenomena.- The unsteady one-dimensional flow equations may be integrated by a characteristic method similar to that used for two-dimensional or three-dimensional rotational symmetric flow. The development of the characteristic method and the equations used are given in reference 8. These characteristic equations are:

$$\frac{\delta_+ P}{\delta \tau} = - \frac{au}{A} \frac{\partial A}{\partial \xi} - \frac{a}{A} \frac{\partial A}{\partial \tau} + a \frac{\delta_+ S}{\delta \tau} + (\gamma - 1)a \frac{DS}{D\tau} + F - \Psi a^{(\gamma-3)/(\gamma-1)} e^{\gamma S} \tag{1}$$

and

$$\frac{\delta_- Q}{\delta \tau} = - \frac{au}{A} \frac{\partial A}{\partial \xi} - \frac{a}{A} \frac{\partial A}{\partial \tau} + a \frac{\delta_- S}{\delta \tau} + (\gamma - 1)a \frac{DS}{D\tau} - F - \Psi a^{(\gamma-3)/(\gamma-1)} e^{\gamma S} \tag{2}$$

where $P = \sigma a + u$, $Q = \sigma a - u$, and F is a body force acting on the fluid. Equation (1) applies along the P-line, whose slope is $u + a$, and equation (2) applies along the Q-line, whose slope is $u - a$. These lines are shown in figure 2, which presents a diagram of the basic characteristic net. The entropy equation

$$\frac{DS}{D\tau} = f(a,u,S,\xi,\tau)$$

applies along the streamline u and is given by the problem conditions.

The term Ψ is defined as the nondimensional value of mass removed per unit length in unit time. This term is related to the geometry and flow characteristics of the inlet in the following fashion. Consider the evaluation of Ψ for the two-dimensional inlet shown in figure 1(c). (A similar consideration could be applied to a circular inlet.) The mass flow rate through unit length of the perforated upper wall of this inlet may be expressed as

$$m_w = \psi w \rho_h c_h$$

where

ψ ratio of open area in wall to total area

w width of inlet (see fig. 1(c))

ρ_h density of fluid in wall opening

c_h local sound speed in wall opening

In the equation for m_w, c_h is equal to $a_h c_\infty$ where c_∞ is the free-stream sonic speed; hence

$$m_w = \psi w \rho_h a_h c_\infty$$

It is shown on page 15 of reference 8, that

$$\rho_h = \rho_\infty a_h{}^\sigma e^{-\gamma S_h}$$

where ρ_∞ is the density for the free-stream condition wherein $a_\infty = 1$. Thus

$$m_w = \psi w \rho_\infty c_\infty a_h{}^{\sigma+1} e^{-\gamma S_h}$$

The term Ψ is given on page 6 of reference 8. In the notation of the present paper,

$$\Psi = \frac{h c_\infty m_w}{\gamma A p_\infty}$$

where p_∞ is free-stream pressure. The term a_h is evaluated by considering that the flow through the holes occurs at its local sonic velocity. This value is obtained by first writing Bernoulli's equation in its nondimensional form, which is

$$\sigma a^2 + u^2 = \text{Constant}$$

If it is considered that the flow expands so that $a_h = a = u$, then

$$\sigma a^2 + u^2 = \sigma a_h{}^2 + a_h{}^2 = (\sigma + 1) a_h{}^2$$

or

$$a_h{}^2 = \frac{\sigma a^2 + u^2}{\sigma + 1}$$

Substituting for m_w and a_h results in

$$\Psi = \frac{h c_\infty}{\gamma A p_\infty} \psi w \rho_\infty c_\infty \left(\frac{\sigma a^2 + u^2}{\sigma + 1} \right)^{(\sigma+1)/2} e^{-\gamma S_h}$$

Note that

$$\frac{\gamma p_\infty}{\rho_\infty} = c_\infty{}^2 \qquad\qquad wh = A_\infty$$

so that

$$\Psi = \psi \frac{A_\infty}{A}\left(\frac{\sigma a^2 + u^2}{\sigma + 1}\right)^{(\sigma+1)/2} e^{-\gamma S_h}$$

With the substitution of $\gamma = \frac{\sigma + 2}{\sigma}$,

$$a^{(\gamma-3)/(\gamma-1)} = \left(\frac{1}{a}\right)^{\sigma-1}$$

Hence the term $\Psi a^{(\gamma-3)/(\gamma-1)} e^{\gamma S}$ of equations (1) and (2) may be expressed in terms of geometry and flow properties as

$$\psi \frac{A_\infty}{A}\left(\frac{\sigma a^2 + u^2}{\sigma + 1}\right)^{(\sigma+1)/2} \frac{1}{a^{\sigma-1}}$$

The treatment of tunnels with other shapes or with different perforation distributions may change the area factor of this equation. For instance, if the inlet is assumed to be circular with perforations over the entire area and the entrance diameter is considered the unit length, then A_∞/A in the above equation must be replaced with $4\sqrt{A_\infty/A}$.

The term $(\gamma - 1)a \frac{DS}{D\tau} \pm F$ is shown on page 49 of reference 8 to contribute the following to the value of Δ_+P and Δ_-Q, respectively:

$$F\left[1 - (\gamma - 1)\frac{u}{a}\right]\Delta_+\tau + a\,\Delta_+S$$

and

$$-F\left[1 + (\gamma - 1)\frac{u}{a}\right]\Delta_-\tau + a\,\Delta_-S$$

where

$$F = -\frac{\lambda h}{2d} u^2 \frac{u}{|u|}$$

Here d is the diameter of an area equivalent to the cross-sectional area of the inlet, or $d = \sqrt{\frac{4}{\pi} A}$, and λ is a solution of the following equation:

$$\frac{1}{\lambda^{1/2}} = 2 \log_{10} \frac{ud}{\nu} \lambda^{1/2} - 0.8$$

where ν is the kinematic viscosity. The terms Δ_+S and Δ_-S can be evaluated once the entropy is determined.

The determination of the entropy proceeds in this manner. The value of the entropy is already known at the previously calculated points B and C of figure 2. It is desired to

calculate the entropy at the unknown point D. The rate of change of entropy along the streamline of slope u from the point T located on line BC to the point D is given by

$$\frac{DS}{D\tau} = -\frac{uF}{a^2}$$

This value may be calculated at T by interpolations of the values at B and C and at the point D after a and u are estimated or calculated at that point. The value of S at D is then determined from the relation

$$S_D = S_T - \left[\left(\frac{uF}{a^2}\right)_T + \left(\frac{uF}{a^2}\right)_D\right]\frac{\tau_D - \tau_T}{2}$$

where the subscripts T and D indicate the values of the respective variables at points T and D. Once S_D is known, then

$$\Delta_+S = S_D - S_B$$

and

$$\Delta_-S = S_D - S_C$$

where the subscripts B and C indicate the values of the variables at points B and C. After these modifications have been completed, equations (1) and (2) can be written in the delta form:

$$\Delta_+P = -\frac{a}{A}\left(u\frac{\partial A}{\partial \xi} + \frac{\partial A}{\partial \tau}\right)\Delta_+\tau - \frac{\psi A_\infty}{A}\left(\frac{\sigma a^2 + u^2}{\sigma + 1}\right)^{(\sigma+1)/2}\frac{1}{a^{\sigma-1}}\Delta_+\tau + F\left(1 - \frac{(\gamma - 1)u}{a}\right)\Delta_+\tau + a\,\Delta_+S \tag{3}$$

and

$$\Delta_-Q = -\frac{a}{A}\left(u\frac{\partial A}{\partial \xi} + \frac{\partial A}{\partial \tau}\right)\Delta_-\tau - \frac{\psi A_\infty}{A}\left(\frac{\sigma a^2 + u^2}{\sigma + 1}\right)^{(\sigma+1)/2}\frac{1}{a^{\sigma-1}}\Delta_-\tau - F\left(1 + \frac{(\gamma - 1)u}{a}\right)\Delta_+\tau + a\,\Delta_-S \tag{4}$$

The application of these equations to an actual flow field is seen upon consideration of figure 2. Assume that the flow properties a, u, and S are known at both of the points B and C. It is desired to determine the flow at point D from the known data. The point D may be located by the intersection of the lines of slope, $u + a$ extending from point B, and $u - a$ extending from point C. Then the equation for $\delta_+P/\delta\tau$ is integrated along the $u + a$ line and the equation for $\delta_-Q/\delta\tau$ is similarly integrated along the $u - a$ line, to give the new values of P and Q at the point D. A third point T is interpolated between B and C so that a line of slope u extending from T will intersect D. The entropy equation is then integrated along that line to obtain the final values of a, u, and S.

The integrations are actually computed by writing the differential equations in a delta form. Then

$$\left.\begin{aligned} P_D &= P_B + \Delta_+P = P_B + \left(\frac{\delta_+P}{\delta\tau}\right)_B(\tau_D - \tau_B) \\ Q_D &= Q_C + \Delta_-Q = Q_C + \left(\frac{\delta_-Q}{\delta\tau}\right)_C(\tau_D - \tau_C) \end{aligned}\right\} \tag{5}$$

and

$$S_D = S_T + \Delta S = S_T + \left(\frac{DS}{D\tau}\right)_T(\tau_D - \tau_T)$$

where the subscripts refer to points in figure 2. Using the characteristic equations in this form permits the evaluation of P_D and Q_D. Once these are known, a and u may be determined from the simultaneous equations

$$\sigma a_D + u_D = P_D$$

$$\sigma a_D - u_D = Q_D$$

or

$$a_D = \frac{P_D + Q_D}{2\sigma}$$

$$u_D = \frac{P_D - Q_D}{2}$$

The values of ξ, τ, a, u, and S for point D can be determined by substituting the corresponding values at points B and C into equations (3) and (4) and performing the indicated computations. However, greater accuracy can be attained if the slope of the characteristic lines is made equal to the average of the slopes at each of the end points, so that the line slope is representative of the slopes at both B and D rather than at B as in the primary computation. Such a consideration of both slopes was met by computing each term of equations (3) and (4), using the appropriate values of A, a, u, S, and so forth, for each of the points B, C, and D. The appropriate values of the terms were then averaged to give the final values of the terms used in equations (3) and (4). The use of these values requires that A_D, u_D, S_D, ξ_D, and τ_D be recomputed several times to insure stable values and thus increase the accuracy of the computation. It was found that about five or six such iterations would determine the value of u_D to within 0.00001.

Equations for shock phenomena.- Normal shocks occur in the inlet as a result of the intersection of either two P-lines or two Q-lines. The primary normal shock which is necessary to satisfy the initial conditions of the inlet flow is the result of the intersection of the supersonic and subsonic Q-lines. Other shocks may exist on either side of

the primary shock and are usually much weaker unless a sudden shock-type change is made at either the entrance or the exit of the inlet. This study is interested primarily in the control of the motion of the primary shock, as such motion can have serious effects on the flow properties of the inlet, especially if unstarting of the inlet is involved.

The motions of either the primary shock or the subsequently formed secondary shocks are computed by using the equations and, to a varied extent, the methods given in reference 8. These equations are applied to the field shown in figure 3(a), which represents a typical Q-shock characteristic diagram. A magnified portion of figure 3(a) is shown in figure 3(b).

The discussion in reference 8 shows that P- and Q-shocks have respectively different values of P or Q on each side of the shock. This is expected because the two P- or Q-lines which intersect on the shock surface will not have the same value of P or Q. The shock properties, that is, Mach number, velocity, and strength, are primarily dependent on the value of Δ_+P or Δ_-Q which occurs across the shock. Hence it is necessary to compute the value of Δ_+P or Δ_-Q across the shock before its properties can be determined. The computation of a Q-shock proceeds somewhat in the following manner. In figure 3(b), the values of a, u, and S in the flow field at the characteristic points A and C are known, as well as the values at the points B_f and B_r (in front of and at the rear of the shock). It is now desired to compute a, u, S, ξ, and τ at the points Z_f and Z_r (the front and rear sides of the shock point Z).

The shock point is approximately located by computing the location of the intersection of the P-line from A and the shock from B, using the shock velocity W for the slope of the shock. Then the value of P at Z_f may be computed from equation (3), and by using the interpolated point E whose Q-line intersects the point Z_f, it is possible to compute the value of Q at Z_f. These input values P_f and Q_f are then used to determine a_f and u_f. The interpolated point G may be used similarly to compute Q_r, but P_r cannot be computed. Hence it is now necessary to resort to the shock equations relating the shock Mach number and Δ_-Q or Δ_+P. The equation for ΔQ across a Q-shock may be expressed as

$$\Delta Q = Q_r - Q_f = \sigma a_r - u_r - \sigma a_f + u_f$$

It is shown in reference 8 that

$$u_f = W_f + a_f M_{s,f}$$

$$u_r = W_r + a_r M_{s,r}$$

where $M_{s,f}$ is the Mach number of the flow into the shock relative to the shock and $M_{s,r}$ is the Mach number of the flow away from the shock relative to the shock. Then

$$\frac{\Delta Q}{a_f} = \sigma\left(\frac{a_r}{a_f} - 1\right) - \frac{a_r}{a_f} M_{s,r} + M_{s,f} \tag{6}$$

The substitution of σ for $\frac{2}{\gamma - 1}$ into equations (95) and (96) of reference 9 results in

$$\frac{a_r}{a_f} = \frac{\left[(\sigma + 2)M_{s,f}^2 - 1\right]^{1/2}\left(M_{s,f}^2 + \sigma\right)^{1/2}}{(\sigma + 1)M_{s,f}}$$

and

$$M_{s,r} = \left[\frac{M_{s,f}^2 + \sigma}{(\sigma + 2)M_{s,f}^2 - 1}\right]^{1/2}$$

respectively. The substitution of these relations into equation (6) leads to

$$\frac{\Delta Q}{a_f} = \sigma\left\{\frac{\left[(\sigma + 2)M_{s,f}^2 - 1\right]^{1/2}\left(M_{s,f}^2 + \sigma\right)^{1/2} + M_{s,f}^2 - (\sigma + 1)M_{s,f} - 1}{(\sigma + 1)M_{s,f}}\right\} \tag{7}$$

The value of $\Delta P/a_f$ across a P-shock can be found in like manner.

Equation (7) may be solved for $M_{s,f}$ by using an iteration technique such as the Newton-Raphson. Once $M_{s,f}$ is known, a_r may be computed and then u_r may be determined from the shock velocity equation; that is, for a Q-shock

$$u_r = W + a_r M_{s,r}$$

where $M_{s,r}$ is the shock Mach number behind the shock which corresponds to $M_{s,f}$ in front of the shock and is determined from the relation

$$M_{s,r} = \left[\frac{M_{s,f}^2 + \sigma}{(\sigma + 2)M_{s,f}^2 - 1}\right]^{1/2}$$

Thus, the complete properties of the shock may be determined. As with the characteristics, the various velocities may be averaged and a new shock value may be determined. This process may be iterated to the desired degree of accuracy. The P-shocks may be computed in a similar fashion, that is, by first determining P_f, Q_f, and P_r from appropriate known points. Then the shock properties may be determined from corresponding shock equations. However, the shock velocity relations for the P-shock are

$$W = u_f + a_f M_{s,f} = u_r + a_r M_{s,r}$$

A problem that may occur, especially in computation of Q-shocks, is the problem of multiple intersections of the shock and the Q characteristic lines. An example is shown in figure 4. In this figure the shock point Z would normally be computed from the known points A_2, B_2, and S_1, and Q_r would be obtained from an interpolated point occurring between S_1 and C_1. However, it is seen that the Q-lines from B_3, B_4, B_5, C_1, C_2, and C_3 and the shock from S_2 all intersect with the shock from S_1 before that shock intersects with the characteristic line P_2. Although it is possible to search out, test for, and calculate each separate intersection, the process would greatly complicate the program. This complexity may be avoided by obtaining the Q_f value from interpolation between the points A_2 and $S_{1,f}$. The value of Q_r needed to complete the shock point computation is obtained by checking each pair of points $(S_{1,f},C_1)$, (C_1,C_2), (C_2,C_3), $(C_3,S_{2,f})$, and $(S_{2,r},C_4)$ until two points are found for which a Q-line originating at Z_r will intersect the line between the two points. Once this condition is discovered, Q_r may be calculated and the shock values at Z may be determined. Although this method is not quite as exact as the method of computing each intersection, the errors involved should be small and involve only slight changes in shock location. Only small errors are expected because the values of P_f, Q_f, and Q_r are determined from practically the same characteristic lines regardless of the shock-characteristic intersections that occur in between.

Input data for program.- The computing program allows a number of input variations, such as time variation of velocity, pressure, or mass flow at the engine face; time variation of the engine-face area with choked flow assumed at that point; time variation of sonic speed or flow velocity at the inlet entrance; or a possible time variation of the area distribution of the inlet. Several time-variation functions are included. These are steady state, sinusoidal variation, stall, exponential ramp, linear ramp, flat-top impulse, and a triangular-shaped impulse. Any of these are available through a data card. The area derivative and the inlet wall perforation distributions are entered as tabular data. A cubic interpolation routine is used to interpolate the area distributions, whereas a linear routine is used to interpolate the perforation distribution. The linear distribution is used for the perforation table because the values of this distribution may change too abruptly for cubic interpolation. A given value of γ, the ratio of specific heats, may be entered into the program. No provision is made for the variation of its value as this program is more concerned with the effects of external influences which may be used to control the inlet flow properties.

Only one inlet was considered for analysis. This inlet was an internal-compression inlet with an area ratio reduction from 1.0 at the entrance to 0.30 at the throat. It was derived, with modification for friction effects, from a two-dimensional characteristic computation of a supersonic diffuser which would reduce the Mach number of the flow from 3.0 to 1.3. Several small linear area adjustments were made to the area distribution until the

flow could be computed without choked phenomena occurring. A linear subsonic diffuser with a slope of 0.08497 was added to the supersonic portion. The area distribution of this inlet is presented in figure 5.

It was found necessary to fix the dimensions of the inlet if viscous effects were to be computed. The entrance height was assumed to be 1 meter, and the operating altitude was assumed to be 20 000 meters.

Several perforation distributions were considered. A wall with no perforation was used for comparison. Walls with 20 percent and 40 percent perforation from the entrance to station 4.4 were investigated first. Analysis of steady-state flow computations with the shock located at various points along the inlet showed that these distributions would not always permit the shock to remain stationary at any point in the inlet. Hence a third distribution (fig. 5) was determined by trying and modifying perforation distributions until a distribution was attained that would allow the shock to be set at any point in the inlet. A shock located ahead of the inlet was treated in the following fashion. The inlet was considered to be extended forward into the flow sufficiently to be ahead of the shock. The perforation of this portion of the inlet was considered to be zero if the flow was supersonic and equal to 1 or fully open if the flow was subsonic. Although more sophisticated means might be used to represent the escaped flow ahead of the inlet, this very rough method has the advantage that no additional programing is necessary. Also, once the shock is expelled, its exact position is not important. Although some errors will occur in shock position and possibly in time to restart, they will not seriously affect the purpose of the analysis.

RESULTS AND DISCUSSION

Because of the nature of the characteristic programs involved, it was possible to select only one particular condition at the engine face and allow it to vary with time. Variations were applied to flow velocity, static pressure, and mass-flow rate. At the inlet entrance either sonic velocity or flow velocity or both could be chosen for transient variation. All of the studies involved in this analysis are concerned with the various engine-face transients. Any time variation desired could be included in the computations by modifying the transient subprogram. Those chosen were steady state, a sinusoidal variation, a stall transient, a ramp throttle change, and several impulse transients, that is, flat-top, triangular, and half-sine-wave. These transients cover most of those of interest in basic inlet control studies.

The results of a number of computations with simulated impulse transients are shown in figures 6 to 10, which present shock position as a function of time for a single half-sine-wave pulse with a duration of 5 time units. The results of the computations for several stall transients and ramp transients are presented in figures 11 to 17.

Shock Motion Due to Half-Sine-Wave Transient

The transient chosen for this portion of the investigation was forced on the inlet by allowing the engine-face condition to vary with the following equations:

$$C_e = C_{SS}(1 + k \sin \omega\tau) \qquad \left(\tau < \frac{\pi}{\omega}\right)$$

$$C_e = C_{SS} \qquad \left(\tau > \frac{\pi}{\omega}\right)$$

where C_e is the imposed engine-face condition, C_{SS} is the steady-state engine-face condition, and k has the magnitude and sign of the transient. Examination of the equation shows that the transient has the form of a half-sine wave, and then conditions return to normal after the transient has passed. The engine-face values of either velocity, pressure, mass flow rate, or choking area were used to furnish the value of C_{SS}.

This transient function was used because it simulates the application of an impulse to the inlet, especially if the duration of the transient is fairly short compared with the duration of the response. The response to this transient therefore simulates the transfer function which exists between the engine-face flow property and the shock motion.

Examination of this response can provide information on properties of the transfer function such as its oscillatory nature, rate of damping, and especially the linearity of the response – that is, the degree to which the response-function amplitudes are proportional to the magnitude of the input coefficient k. The response functions or shock motions due to the application of velocity, mass flow, pressure, or choking-area half-sine-wave transients are presented in figures 6, 7, 8, and 9. Examination of the response functions of the solid-wall inlet (fig. 6(a)) shows that those which are under control (that is, the shock position returned to its initial value) are reasonably similar in shape. The period is observed to increase from 8 units for $k = -0.050$ to 14 units for $k = -0.100$. This increase in period appears not only in this case but also for the perforated-wall cases.

It may also be observed that the position to which the shock finally settles is somewhat different from the initial position of the shock. This change of shock position for the same end conditions is believed to be due to a computing phenomenon as a similar change occurs regardless of which end condition is held steady (fig. 10(a)). The phenomenon is thought to occur because as the computation of the steady-state end condition progresses, the locations and number of the points on the characteristic line change. Such changes can be expected to cause minor changes in the velocity distribution, and hence a slight change in the final steady-state velocity distribution and in the final shock position.

The effects of opening the wall 20 percent in the region between the shock wave and station 4.4 are shown in figure 6(b). The wall perforations increase the value of the maximum amplitude of the transient which can be returned to steady state from 0.10 to about

0.30, and thus permit a much greater range of controlled operation of the inlet. Also the damping of the amplitude of the shock motion has been reduced, as evidenced by the fact that the shock overshoots in the downstream direction on its return to its final steady-state position. The shock is also returned from a position somewhat upstream of the throat, that is, from about station 4.0 to a point beyond station 4.24. The comments concerning linearity and change of period for the solid-wall case apply generally for the 20-percent open walls.

For the transient which was uncontrolled (an amplitude of 0.31), it was observed that a secondary shock was formed downstream of the throat with no characteristic points existing between the two shocks. This large range between computation values could be the reason that the shock does not return to its original position, since all the intervening effects of the inlet dimensions are missing from the computation.

The effects of adding more perforation to the wall, making it 40-percent open to station 4.4, are shown in figure 6(c). Significant noise is observed in the controlled state. Also, the maximum amplitude of input transient that can be controlled has been increased from about 0.30 to 0.50, and the shock returned from a maximum upstream location of about 3.7 units. The first uncontrolled run, an amplitude of 0.60, shows a rather violent oscillation and little damping compared with the controlled cases.

The results of the computation using a velocity transient at the engine face show that bleeding the subsonic flow in the region between the shock and station 4.4 will allow an appreciable increase in the magnitude of the disturbance that can be controlled. The appearance of the curves also indicates that linear transfer functions can be used to represent the relation between a velocity engine-face transient and the shock location as long as the shock location is controlled and the change in period due to larger intensity disturbances is taken into account.

Similar phenomena are observed if either the mass flow rate or the pressure rather than the engine-face velocity is allowed to take the transient variation. The effects of these transients are shown in figure 7 for the mass-flow variations and in figure 8 for pressure variations at the engine face. As with the velocity transient, it is observed that increasing the wall porosity increases the amplitude of the transient that is controllable, from some value less than 0.005 for the solid wall to 0.200 for 20-percent-open and 0.250 for 40-percent-open walls in the case of a mass-flow transient, and correspondingly from 0.050 to 0.175 for the pressure transient. The observation that the shock motion apparently is not controlled, no matter how small the transient, with zero porosity is probably due to the previously discussed fact that the initially calculated steady state is somewhat different from the finally calculated state and is therefore a calculation phenomenon rather than a physical one. Since the mass-flow value to which the flow must return after the transient has passed is set by the initial steady-state calculation, its value is

different from a true steady-state final value. This difference in mass flow is compensated for only by motion of the shock. Hence the shock does not stand still, as would be expected, but moves toward the nose to compensate for the changed end condition.

These unexpected effects of mass-flow transients on the shock location were reconsidered by using another method of controlling mass flow at the engine face. This method consisted of restricting the area at the engine face to such a value that the flow through the engine face would be choked. The time transient could then be applied to the choking area, thereby changing the mass flow in a fashion corresponding to experimental methods of changing mass flow. Several steady-state runs were required before a value of the choking area A_{ch} (see fig. 1(c)) could be selected which would result in an initial shock position reasonably close to 4.4 units. Several of these runs are shown in figure 9(b). It is seen that if A_{ch} is chosen to be equal to 0.284 the shock position settles to a value of 4.467 after a time of about 14. In order to alleviate the effects of the flow adjustment to final steady-state values, the transients were not started until a time of about 12 at the engine face or about 14 at the shock. The results of applying a half-sine-wave transient to vary the choked area at the engine face in a solid-wall tunnel are shown in figure 10(a). It is observed that the transient response is very similar to the response observed for the velocity change (fig. 6(a)). Also, the shock location returns to the value it had at the start of the transient. Thus, none of the irregular shock motions induced by the mass-flow transient are observed.

The effects of applying the half-sine-wave transient to the inlet with distributed perforated wall are shown in figure 10(b). It is seen that the magnitude of the transient for controlled shock motion is extended from about 0.03 to about 0.3. Also, the controlled shock-motion responses are very similar to those observed for the velocity or pressure transients. Again the shock position returns to its original value. However, for $k = 0.4$ the shock does not go out of control but exhibits a new oscillation and a curve of very different shape, indicating the possible introduction of a limit cycle if the shock is held too long in the region ahead of the throat.

Shock Motion Due to Engine Stall

The disturbances to the inlet flow due to engine stalling were simulated by allowing the flow velocity to vary as

$$u = u_{\infty}\left[1 + \frac{k}{2}(1 - \cos \omega\tau)\right] \tag{8}$$

This function reduces periodically the final velocity of the flow in a fashion very similar to that produced by stalling the flow at the engine compressor. Similar disturbances could also be computed for pressure, mass flow, or choked end-area variations. The results of several calculations using equation (8) are presented in figures 11 to 15.

The results of varying the length of the stall from 1 cycle to 6 cycles, with a period of 5 units per cycle or about 60 cycles per second, in an inlet with an entrance height of 1 m are seen in figure 11. For these data, the inlet was 40-percent open from station 0 to station 4.2 and $k = -0.4$. Thus the velocity was dropped to 0.6 its original value at the minimum value of each cycle. Several phenomena may be observed that the shock goes no farther forward than station 3.85. Thus, the shock motion is well controlled. Second, the shock motion has a number of frequencies other than the initially imposed transient frequency, as may be seen by the highly irregular motion of the shock which is indicative of strongly nonlinear phenomena. Third, it is seen that the shock returns to its final steady-state end position within a period or two after the stall is stopped, thus indicating that the subsonic porous wall is adequately controlling the stalled flow.

For comparison, figure 12(a) shows the effect of the stall transient on the shock if the wall is solid. It is seen that the shock is not contained when the amplitude of the disturbance becomes greater than about $k = -0.10$, whereas the perforated walls control the shock motion for values of k equal to -0.4 in figure 11 and even higher, -0.5 and -0.6, in figure 12(b).

A test of the linearity (with k) of these flows is seen in figure 12(b), which shows the results of using k values of -0.5 and -0.6 for 8 cycles. The shapes are generally similar with regard to the location of maximum and minimum amplitudes; however, one curve is not a multiple of the other.

An imposed limit cycle, as observed in figures 9 to 12, is seen more clearly in figure 13, which presents a long-period stall (50 time units). It is seen here that a cycle 12 to 18 units long practically controls the nature of the flow. In fact, the effects of the imposed 50-unit cycle can scarcely be seen. It is observed, though, that with the longer-period transient cycle the flow returns to normal or steady-state values just as quickly as with the shorter-period transient.

Several stall-simulation runs were made at periods of 12 to 18 units and intensities of -0.20 per cycle. The results of these computations are shown in figure 14. The shock response is about the same for all the periods tested. Although a slight maximum is observed at the period of 16 units per cycle, the increase is so slight that no strong resonant phenomena can be claimed for this inlet. Also, as in previous cases the oscillatory shock motion damps out quickly once the forcing function is stopped.

The results of several stall-simulation variations of the choked area at the engine face are shown in figure 15. This figure also shows the formation of a strong oscillation, with weaker shocks that appear to be due to intersection of Q-lines. These weaker shocks appear in most of the runs that have the larger amplitude disturbances. In most cases they were not plotted so as to reduce confusion in the figures and emphasize the normal-shock motion.

Control of Throttle-Chop Phenomena

A change of the throttle setting of an engine causes a transient at the engine face such that the final values of the flow are changed from one steady-state value to another. It is possible to simulate such a transient by causing one of the flow properties u_e, m_e, or p_e at the engine face to experience a ramp-type transient which may be expressed as a linear change of u_e, m_e, or p_e with respect to time from the original steady-state flow value to a new steady-state value that is $(1 + k)$ times the original value. The transient used consisted of a linear portion extending over a time of 40 units, or about one-eighth of a second in an inlet of 1-meter height, after which the flow retained a new constant value.

A variety of cases were investigated. Several velocity ramp transients were run with a solid-wall nozzle in order to establish a basis for comparison. (See fig. 16.) The perforation distribution presented in figure 5 was used for a number of runs with variations in either u_e or the choked area at the engine face. The results of these runs are presented in figures 17 to 19. Figure 16 shows that with solid walls the shock position is bounded for only a very limited change in the value of the engine-face velocity. As would be expected, once the shock is pushed ahead of the throat it moves immediately out of the inlet. This phenomenon occurs for a reduction in velocity of about 3 percent. The addition of the distributed porous wall shown in figure 5 causes remarkable changes in the shock motion. In figure 17 it is seen that reductions of the engine-face velocity by as much as 60 percent ($k = -0.6$) do not cause the shock to leave the interior of the inlet. Even in an extended run, to 200 units rather than 80 units, the shock is contained (fig. 18) to some value greater than $\tau = 200$, or about 0.6 sec in an inlet 1 meter high. The apparent escape of the shock may be due to an accumulation of errors because of the length of the computer run required. However, in either case, the perforated wall used in conjunction with other inlet control systems does allow sufficient time for these systems, such as area distribution change or a bypass door opening, to return the engine-face operating conditions to their original steady-state value.

The question of the existence of this oscillating phenomenon in an actual porous-wall inlet cannot be decided, as the possibility exists that an unstable computing condition is inherent in the computing program. However, in any investigation of this type of inlet it would be well to include instrumentation capable of checking for such oscillations. It is believed probable that whenever the shock is forced ahead of the throat such oscillations can be expected. For example, in figure 9(a), the oscillations are seen to develop even though the end conditions are constant if the shock is started ahead of the throat, whereas no oscillation occurs if the shock is started downstream of the throat. In figure 9(b), with $A_{ch} = 0.324$ and $A_{ch} = 0.284$ the shock position shows no sign of oscillation. It is believed that if computing instabilities existed they would also be evident in

these cases where the shock remains downstream of the throat. The calculated oscillation is therefore believed to give a valid indication of the behavior of an actual perforated supersonic inlet under a throttle-chop velocity disturbance.

Similar phenomena are shown in figure 19, which presents the results of several computations using a ramp variation of the choked area at the engine face. It is seen that the distributed perforated wall controlled the flow for a change in A_{ch} of as much as 0.33. It is also seen that the choked-flow end condition shows the limit cycle strongly when the shock location moves ahead of the throat.

CONCLUDING REMARKS

This paper presents an analysis of the ability of a perforated wall in an internal-compression supersonic inlet to control the motion of the shock due to a variety of transients in the flow values at the engine face. The following remarks are subject to the possible limitations imposed by computing with a finite-increment one-dimensional characteristic system.

1. The use of internal-compression inlets with walls selectively perforated for subsonic flow makes possible containment of the shock within the inlet for much larger engine-face transients than with solid walls.

2. Selectively perforated walls contain the shock ahead of the throat for reduced flow properties at the engine face; however, a limit cycle of roughly constant magnitude is set up by reflection of the waves between the shock surface and the engine face.

3. Some approximation to linearity of responses to impulse-type transients was observed. However, the development of the limit cycle eliminates any appearance of linearity in the responses to longer (nonimpulse) transients when the average shock position is ahead of the inlet throat.

Langley Research Center,
National Aeronautics and Space Administration,
Langley Station, Hampton, Va., May 2, 1969,
720-03-00-02-23.

REFERENCES

1. Anderson, Arthur A.; and Weinstein, Maynard I.: Aerodynamic Performance of Several Techniques for Spike-Position Control of a Blunt-Lip Nose Inlet Having Internal Contraction; Mach Numbers of 0.63 and 1.5 to 2.0. NACA RM E57D15, 1957.

2. Wilcox, Fred A.: Investigation of a Continuous Normal-Shock Positioning Control for a Translating-Spike Supersonic Inlet in Combination With J34 Turbojet Engine. NACA RM E57G16, 1957.

3. Anderson, Bernhard H.; and Bowditch, David N.: Investigation of Inlet Control Parameters for an External-Internal-Compression Inlet From Mach 2.1 to 3.0. NACA RM E58G08, 1958.

4. Whalen, Paul P.; and Wilcox, Fred A.: Use of Subsonic Diffuser Mach Number as a Supersonic-Inlet Control Parameter. NACA RM E56F05, 1956.

5. Wilcox, Fred A.; and Perchonok, Eugene: Aerodynamic Control of Supersonic Inlets for Optimum Performance. NACA RM E55L14, 1956.

6. Evvard, John C.; and Blakey, John W.: The Use of Perforated Inlets for Efficient Supersonic Diffusion. NACA TN 3767, 1956. (Supersedes NACA RM E51B10.)

7. Hunczak, Henry R.; and Kremzier, Emil J.: Characteristics of Perforated Diffusers at Free-Stream Mach Number 1.90. NACA RM E50B02, 1950.

8. Rudinger, George: Wave Diagrams for Nonsteady Flow in Ducts. D. Van Nostrand Co., Inc., c.1955.

9. Ames Research Staff: Equations, Tables, and Charts for Compressible Flow. NACA Rep. 1135, 1953. (Supersedes NACA TN 1428.)

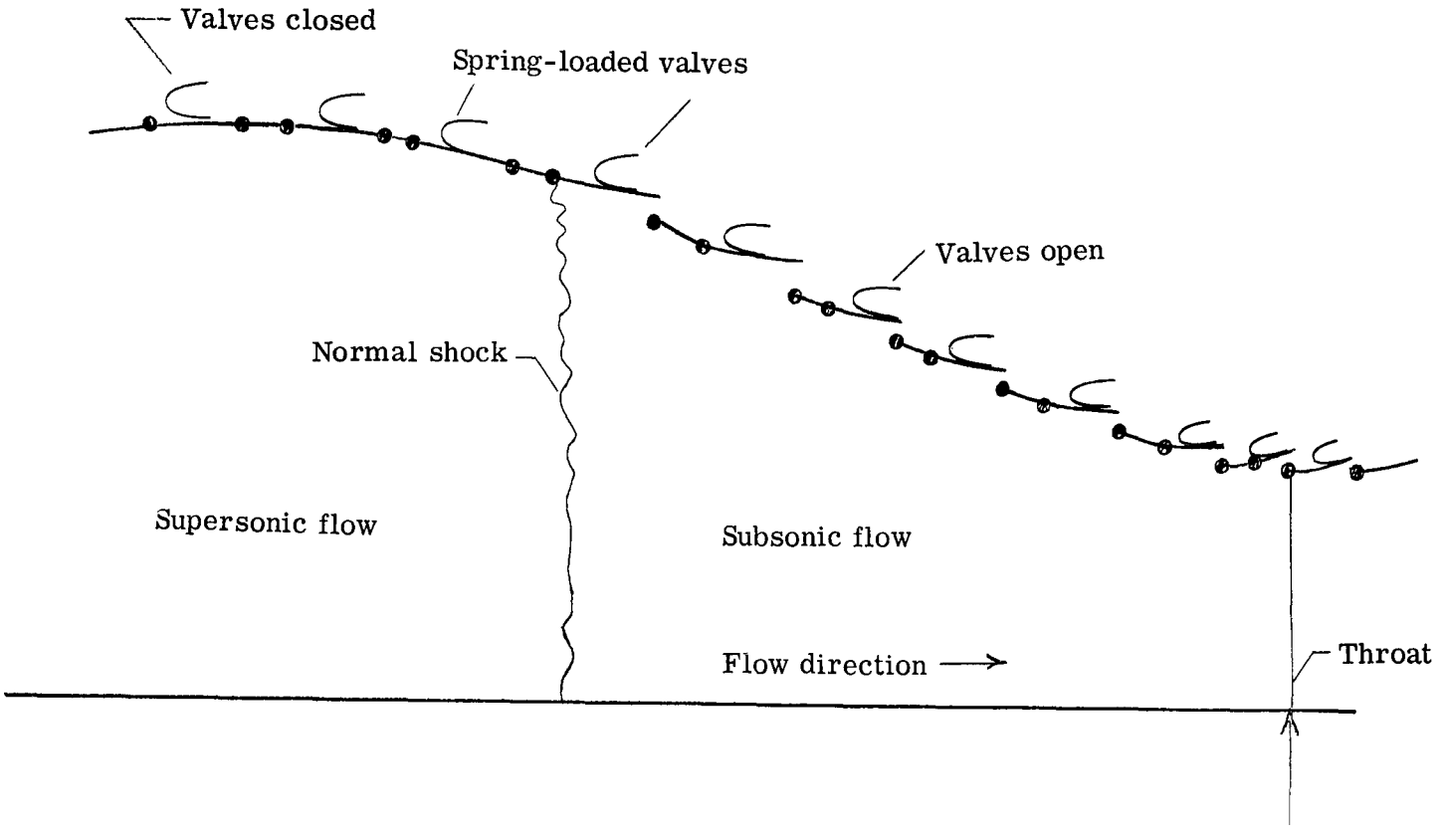

(a) Design of the perforated wall.

Figure 1.- Inlet design.

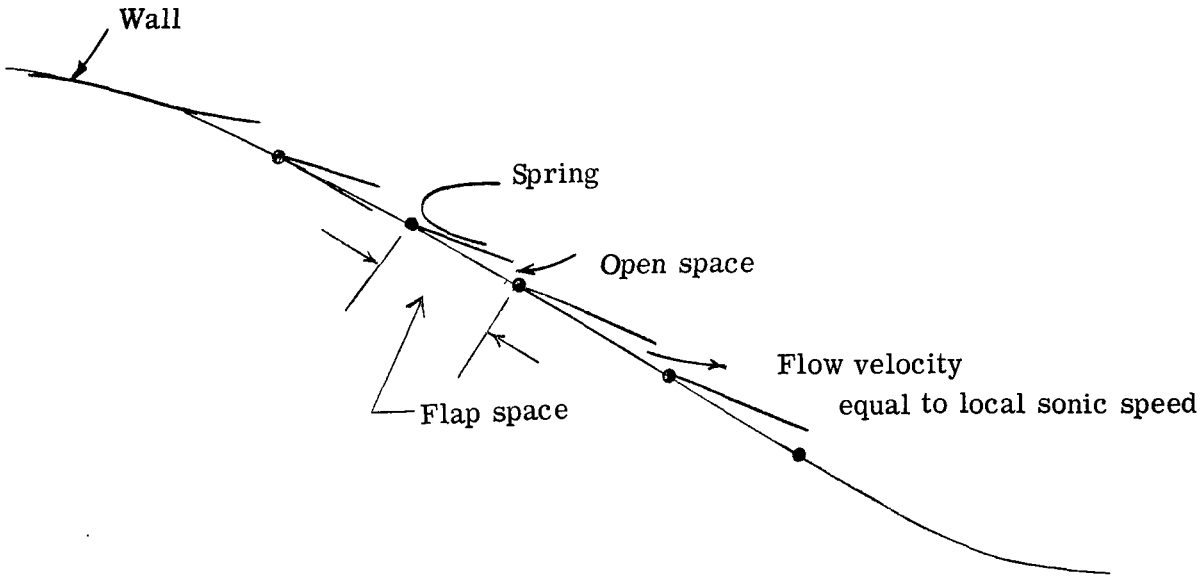

Subsonic pressure opens flapper valves

Springs close valves for supersonic flow

(b) Structure of perforated wall considered for control of shock position.

Figure 1.- Continued.

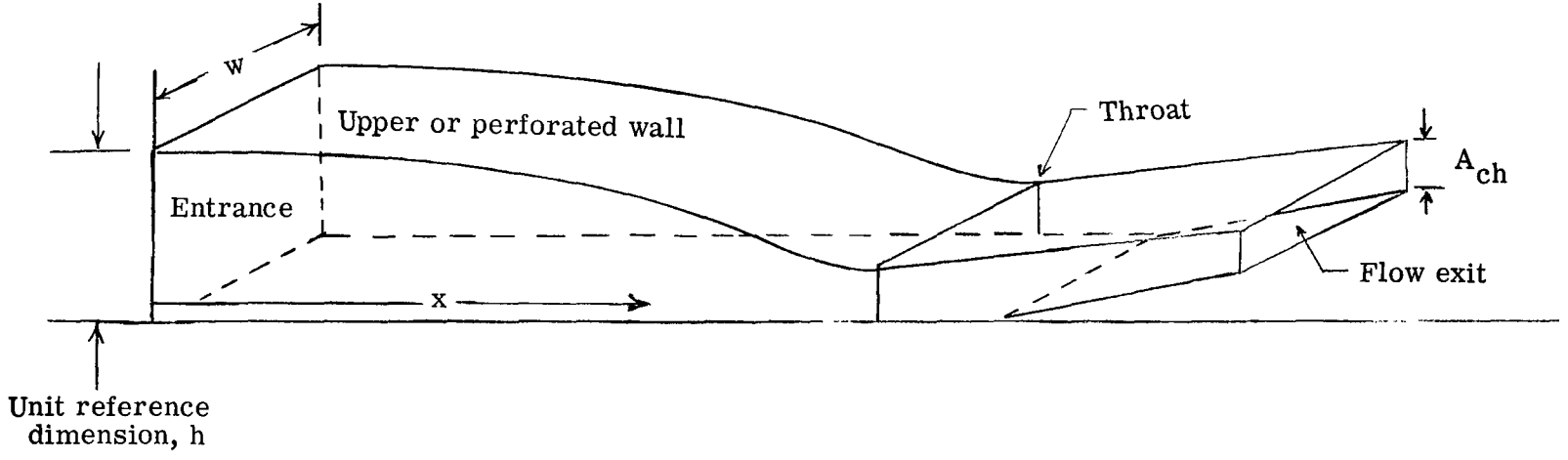

(c) Diagram showing variable-area choked-flow end condition at engine face.

Figure 1.- Concluded.

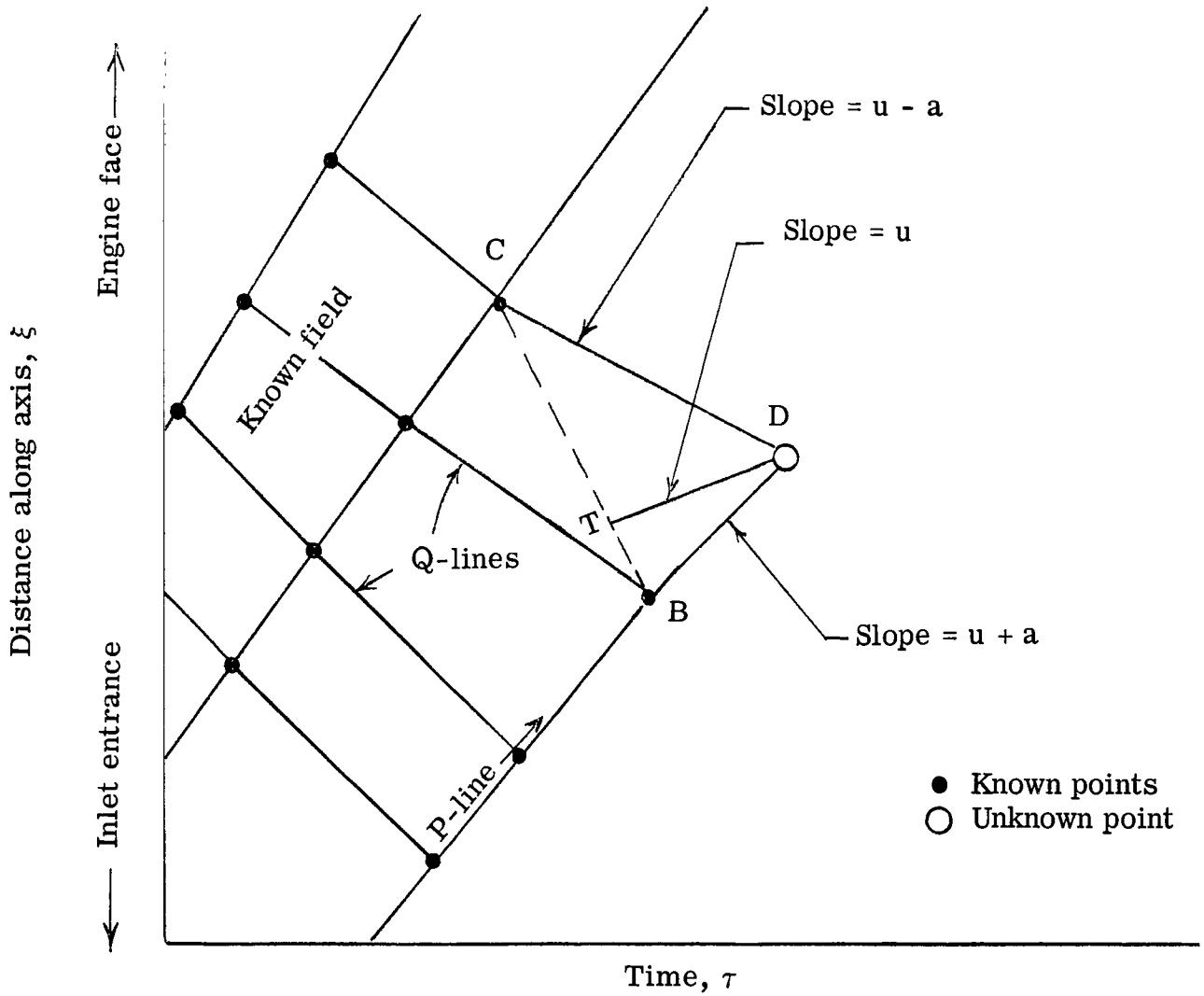

Figure 2.- Diagram of basic characteristic network.

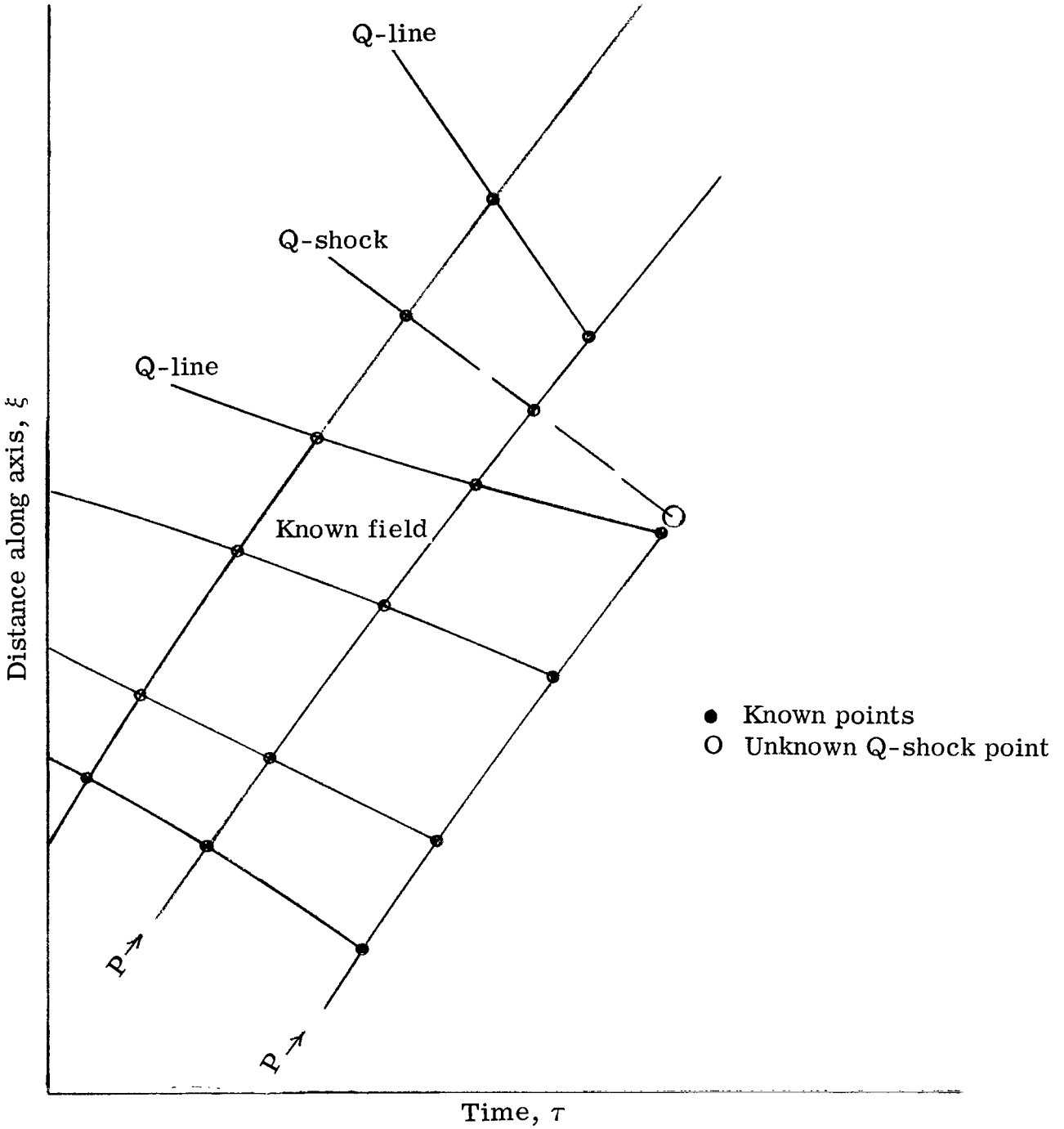

(a) Sketch showing Q-line intersection to form Q-shock.

Figure 3.- Q-shock characteristic network.

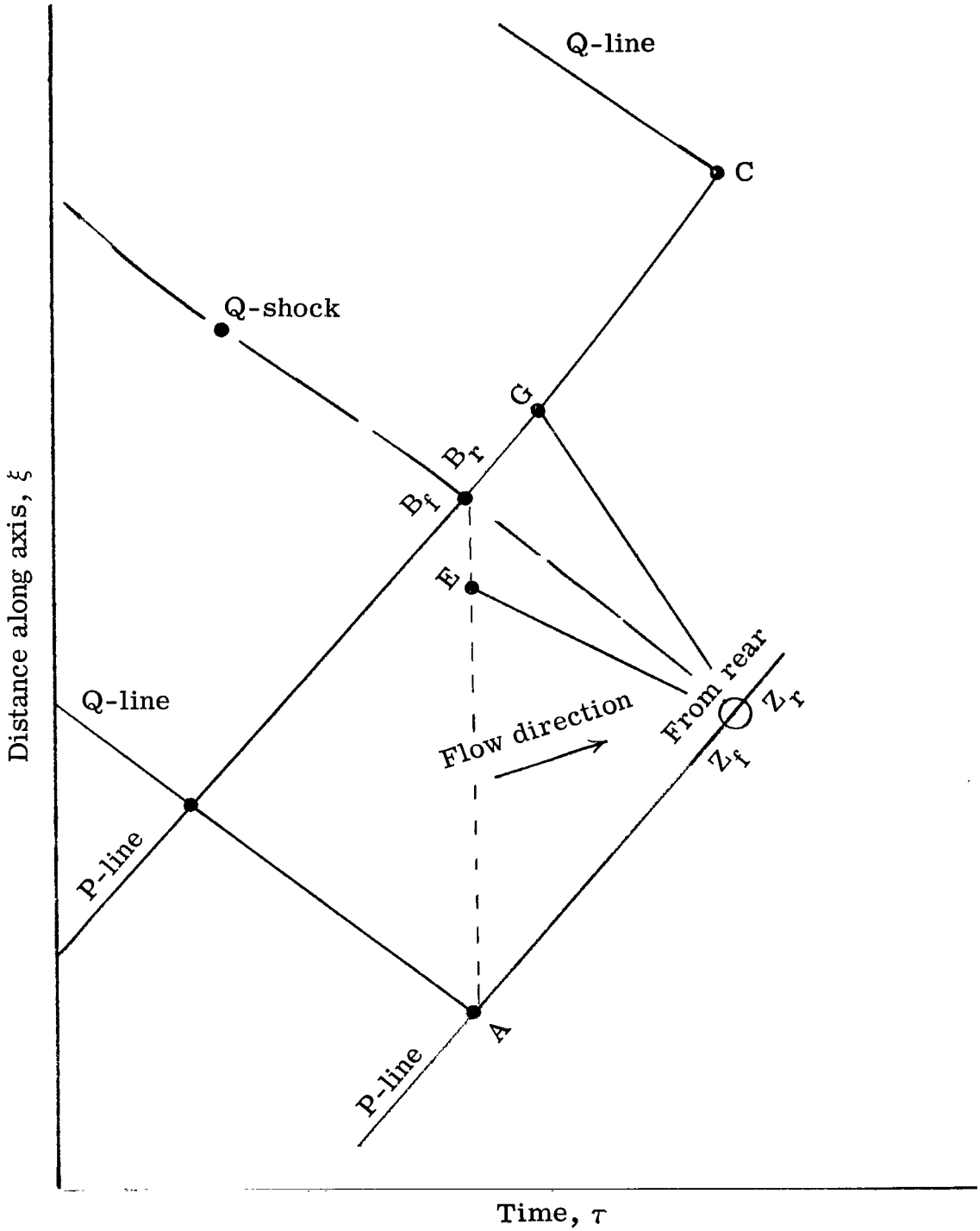

(b) Detailed sketch of a shock point.

Figure 3.- Concluded.

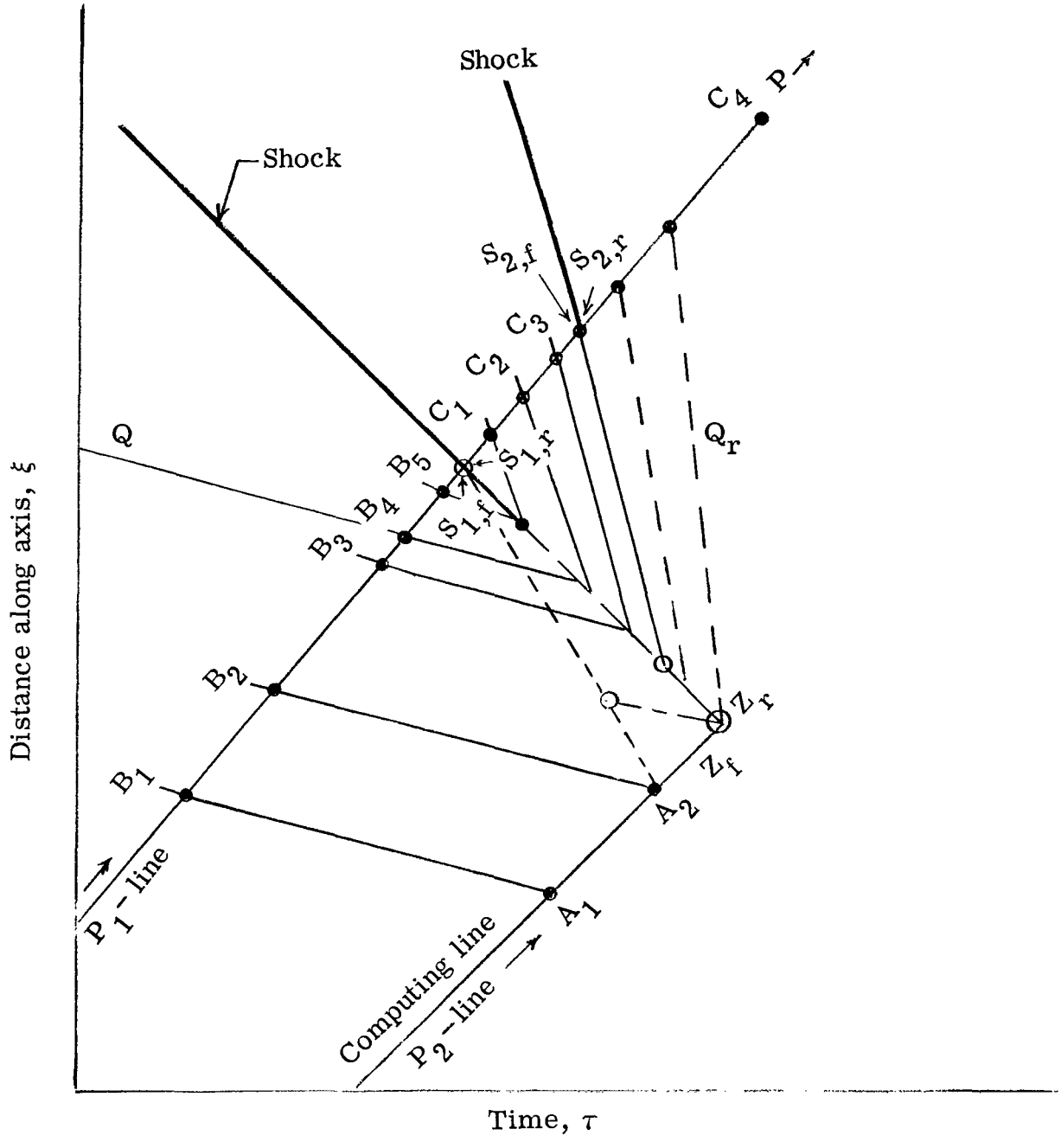

Figure 4.- Multiple characteristic intersections.

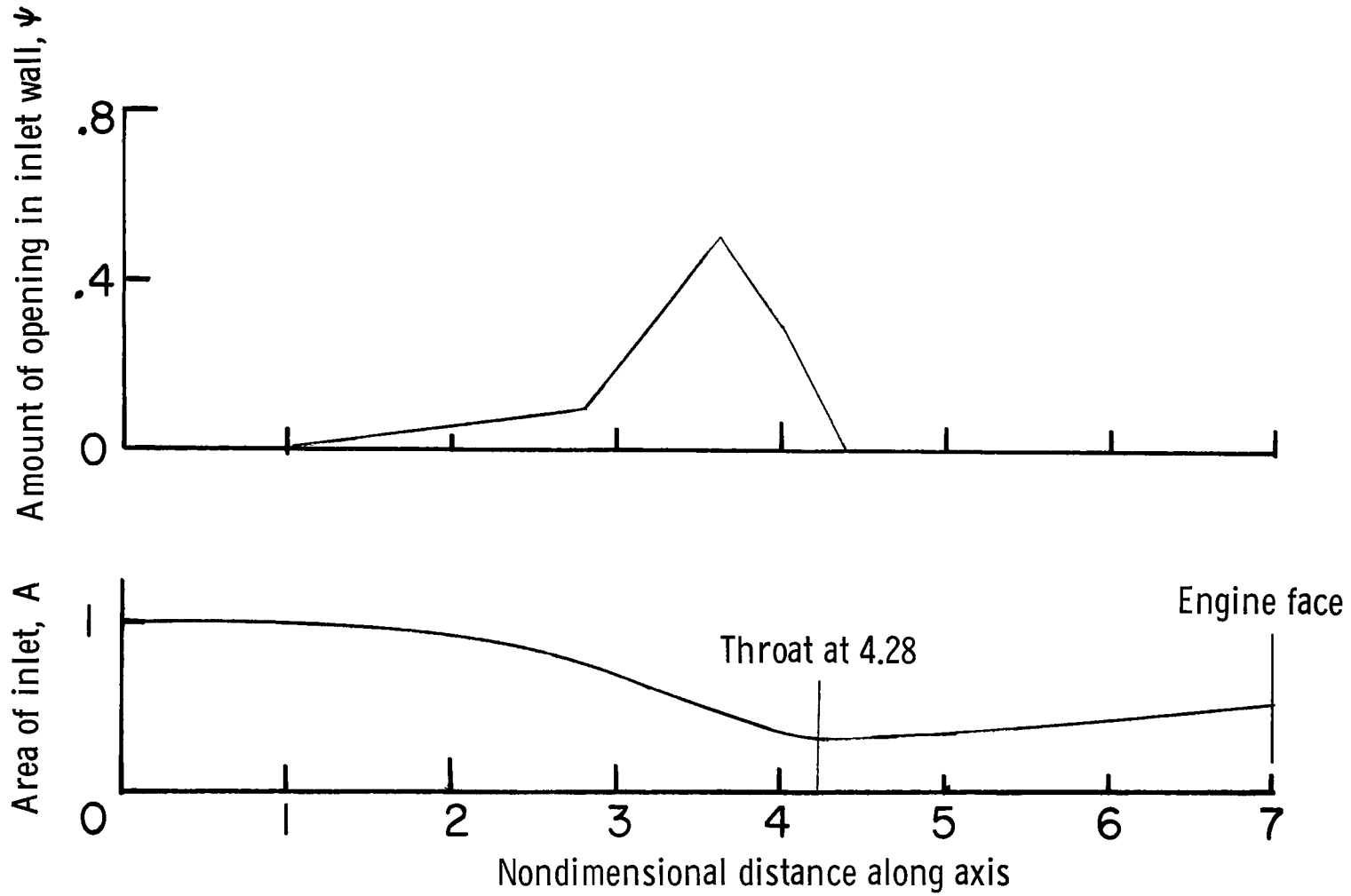

Figure 5.- Distributions of area and perforations (distributed perforated wall) of inlet.

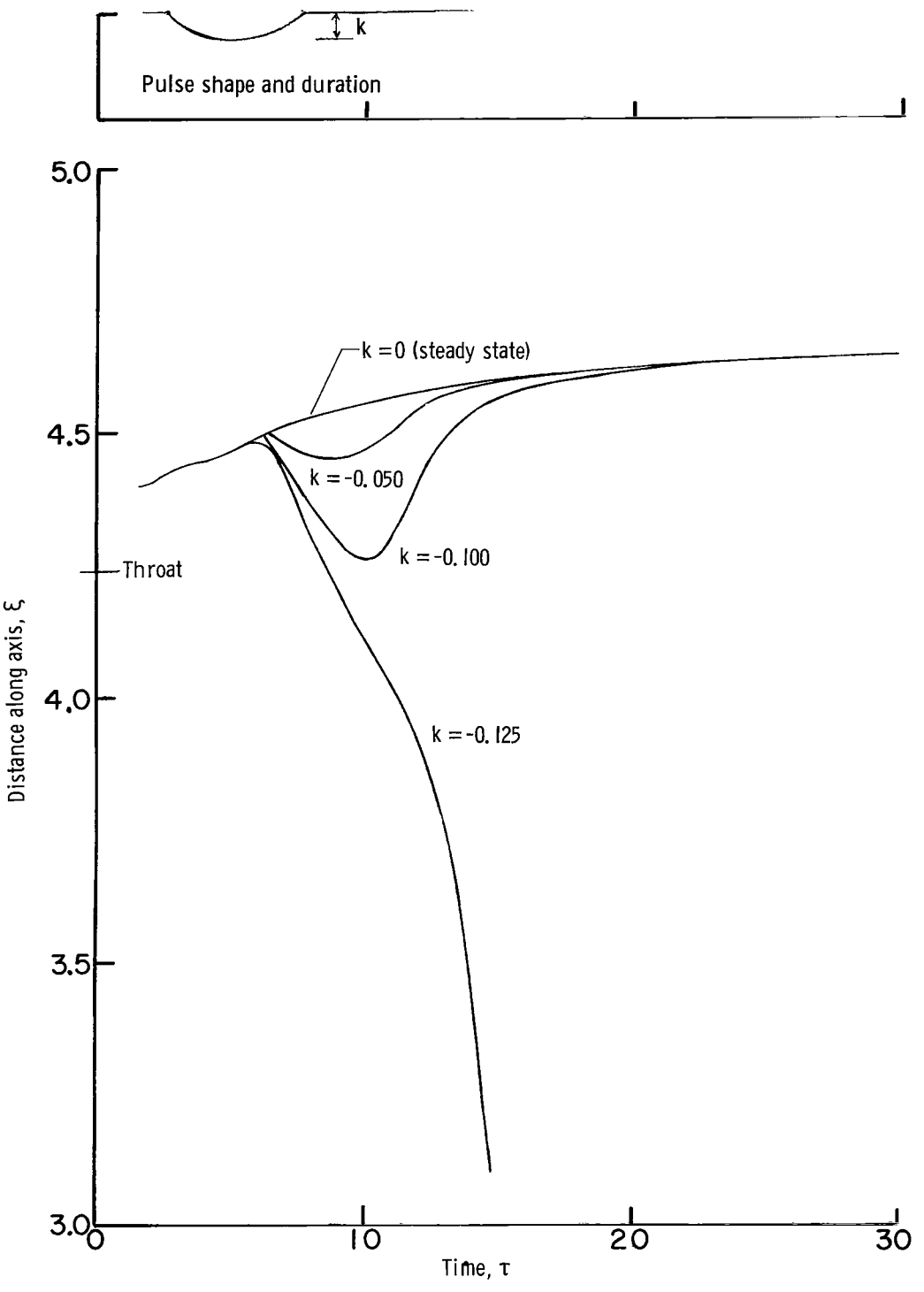

(a) Solid wall.

Figure 6.- Shock motion due to sinusoidal impulse in engine-face velocity.

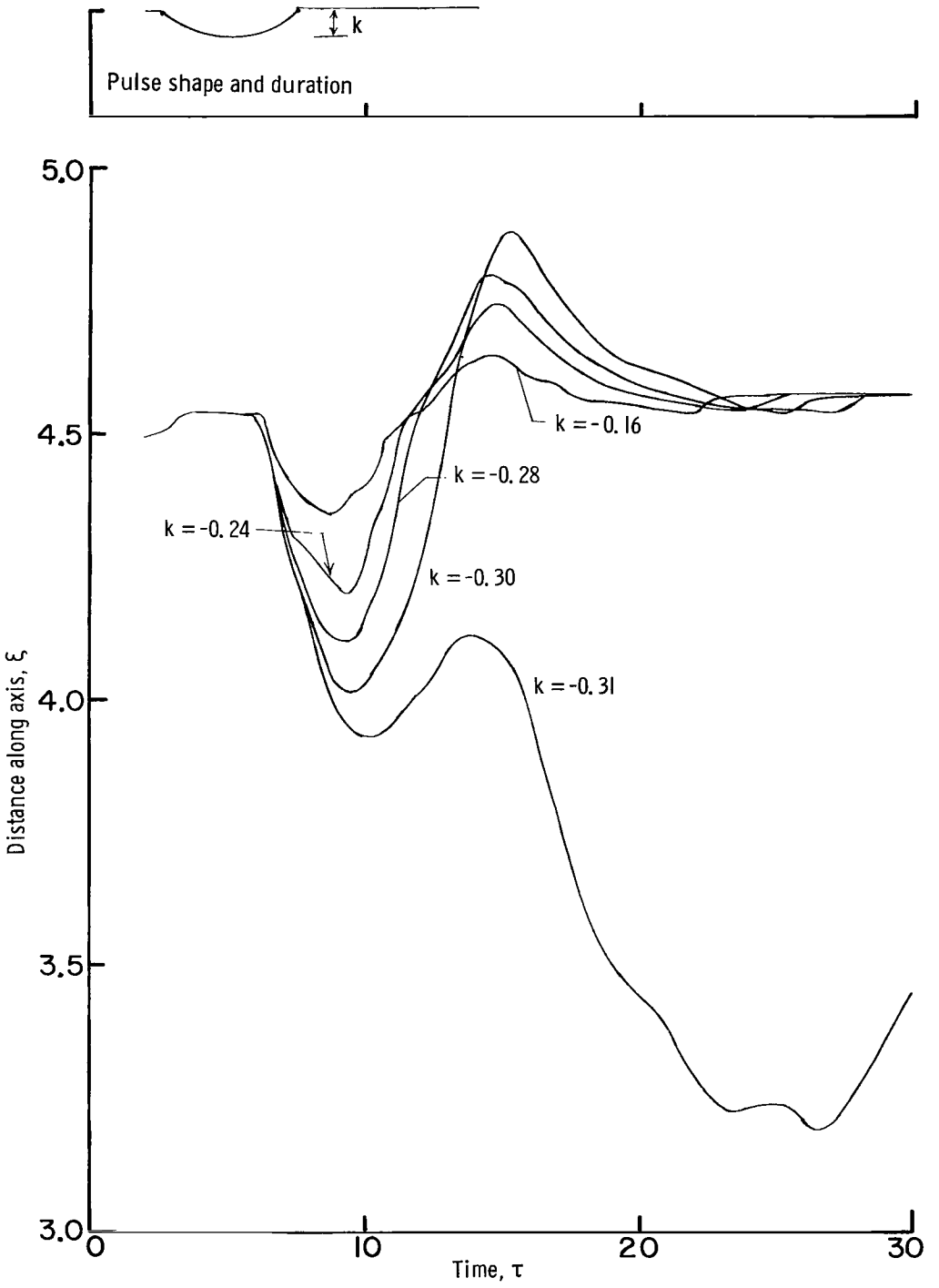

(b) 20-percent perforated wall.

Figure 6.- Continued.

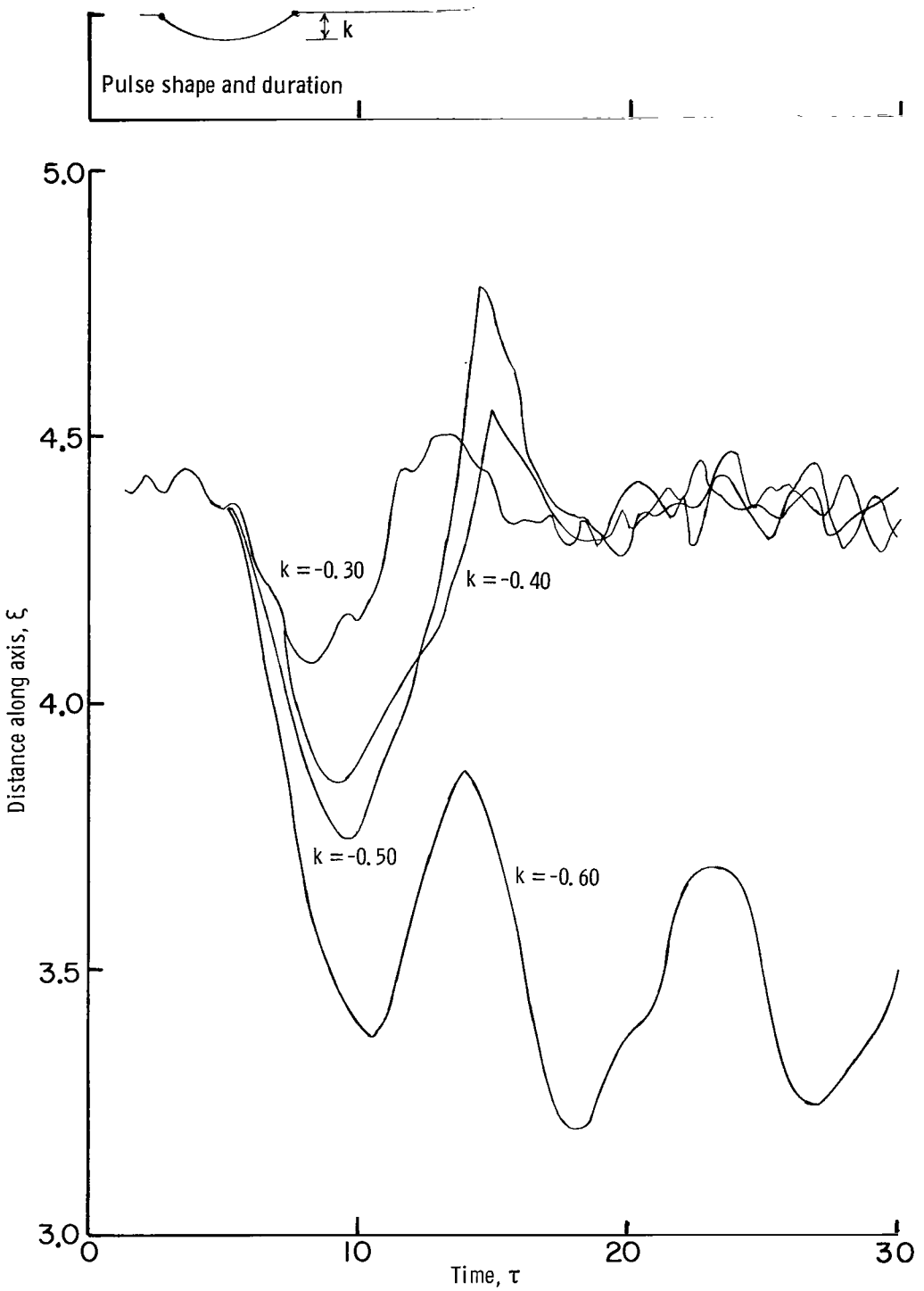

(c) 40-percent perforated wall.

Figure 6.- Concluded.

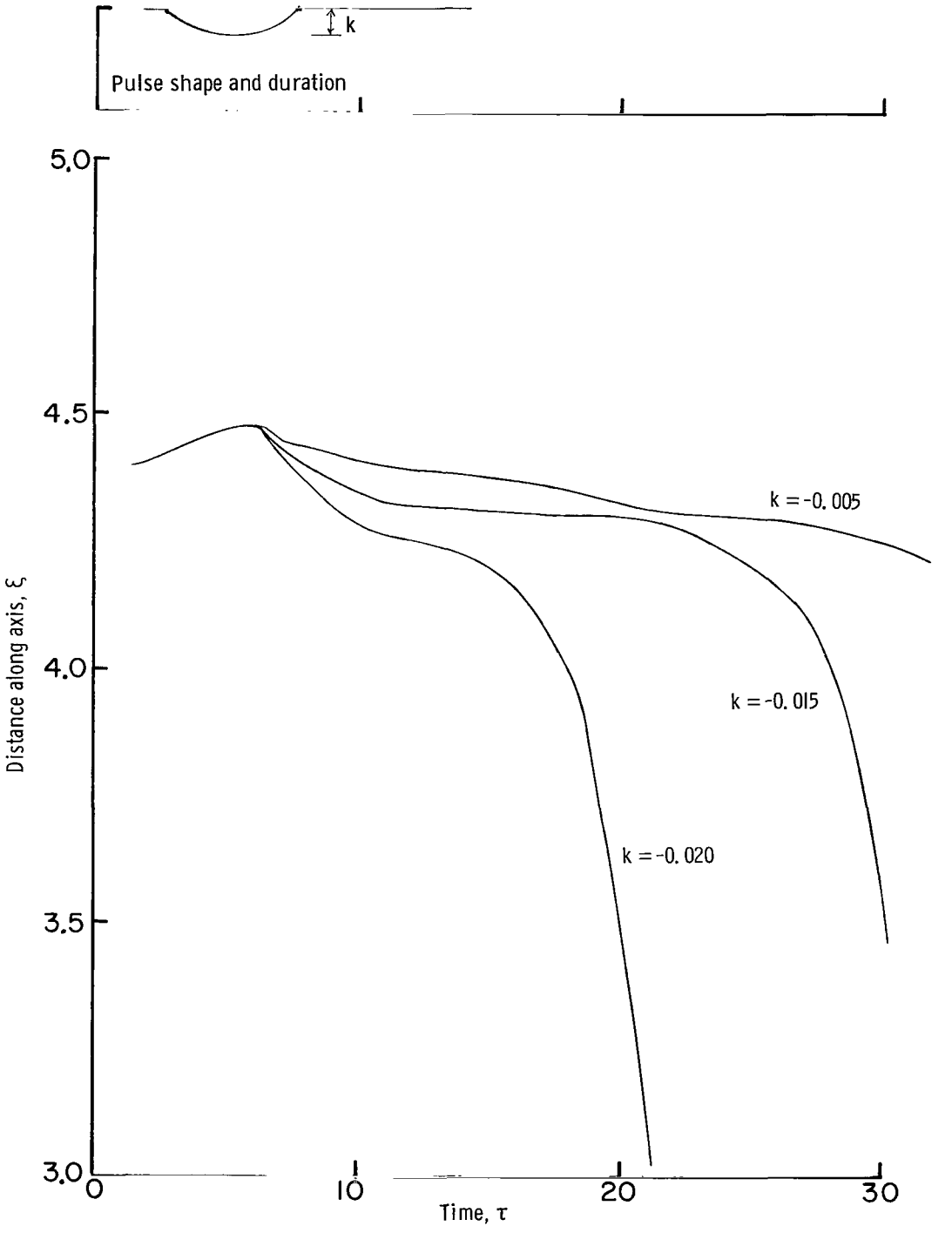

(a) Solid wall.

Figure 7.- Shock motion due to sinusoidal impulse in engine-face mass flow.

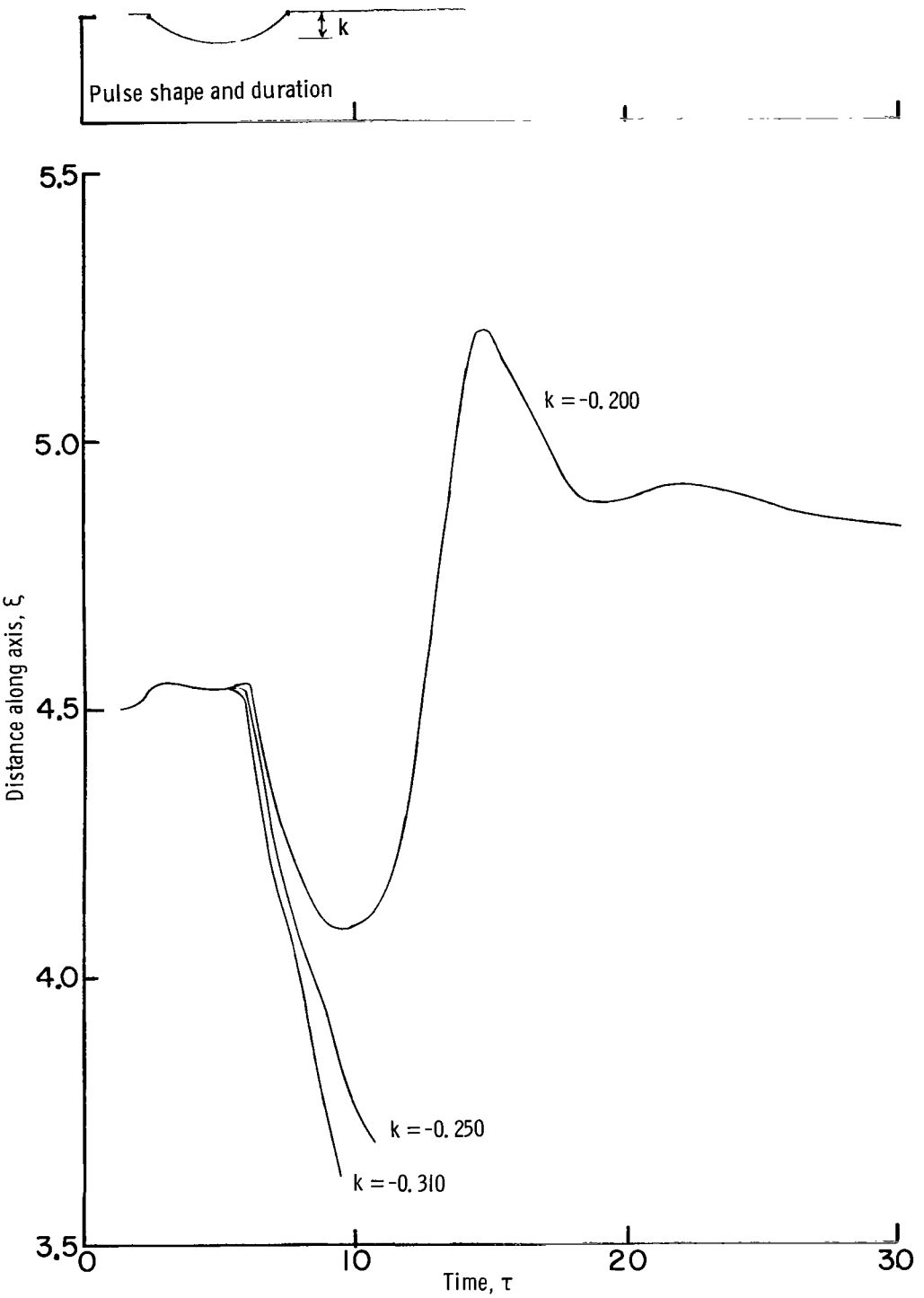

(b) 20-percent perforated wall.

Figure 7.- Continued.

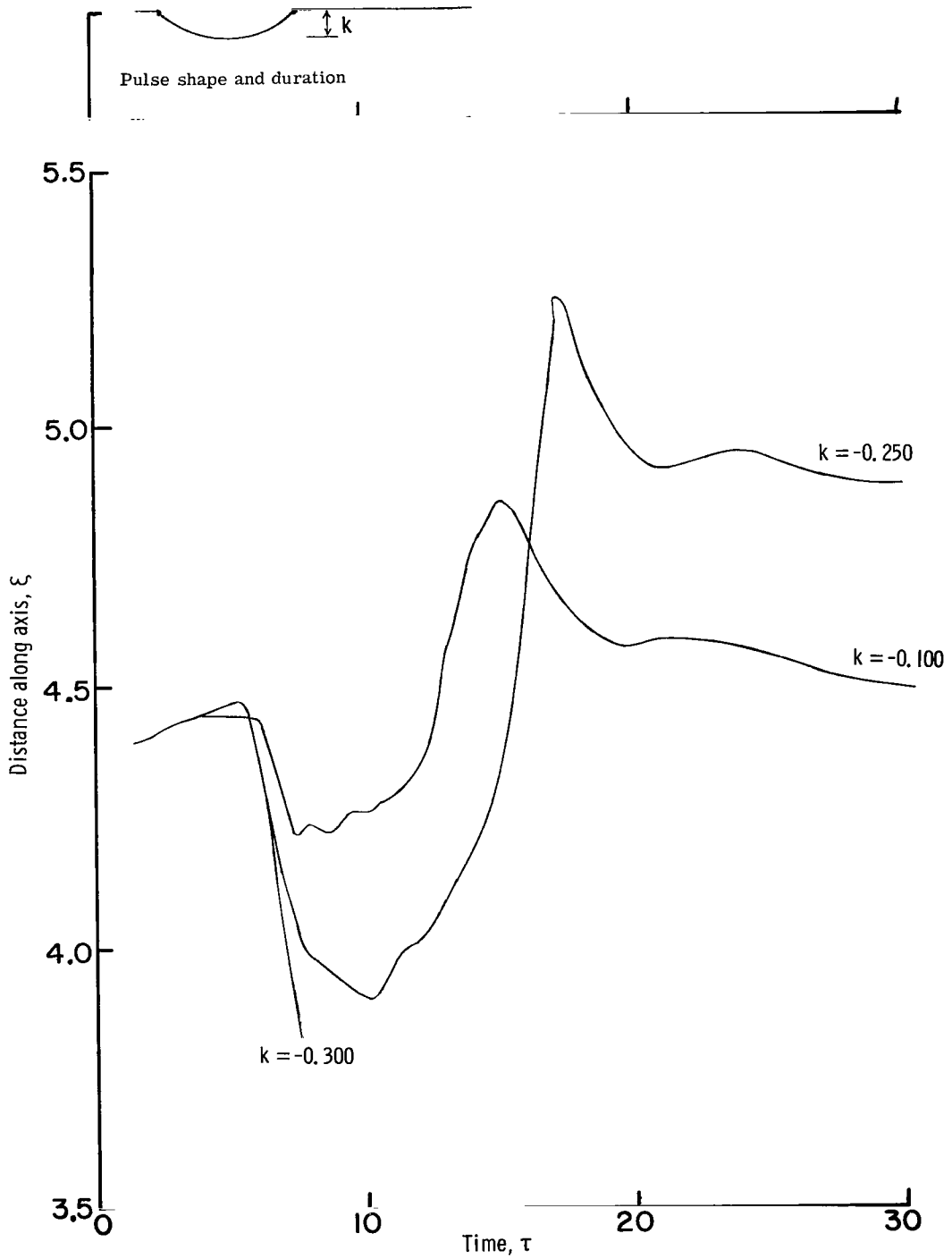

(c) 40-percent perforated wall.

Figure 7.- Concluded.

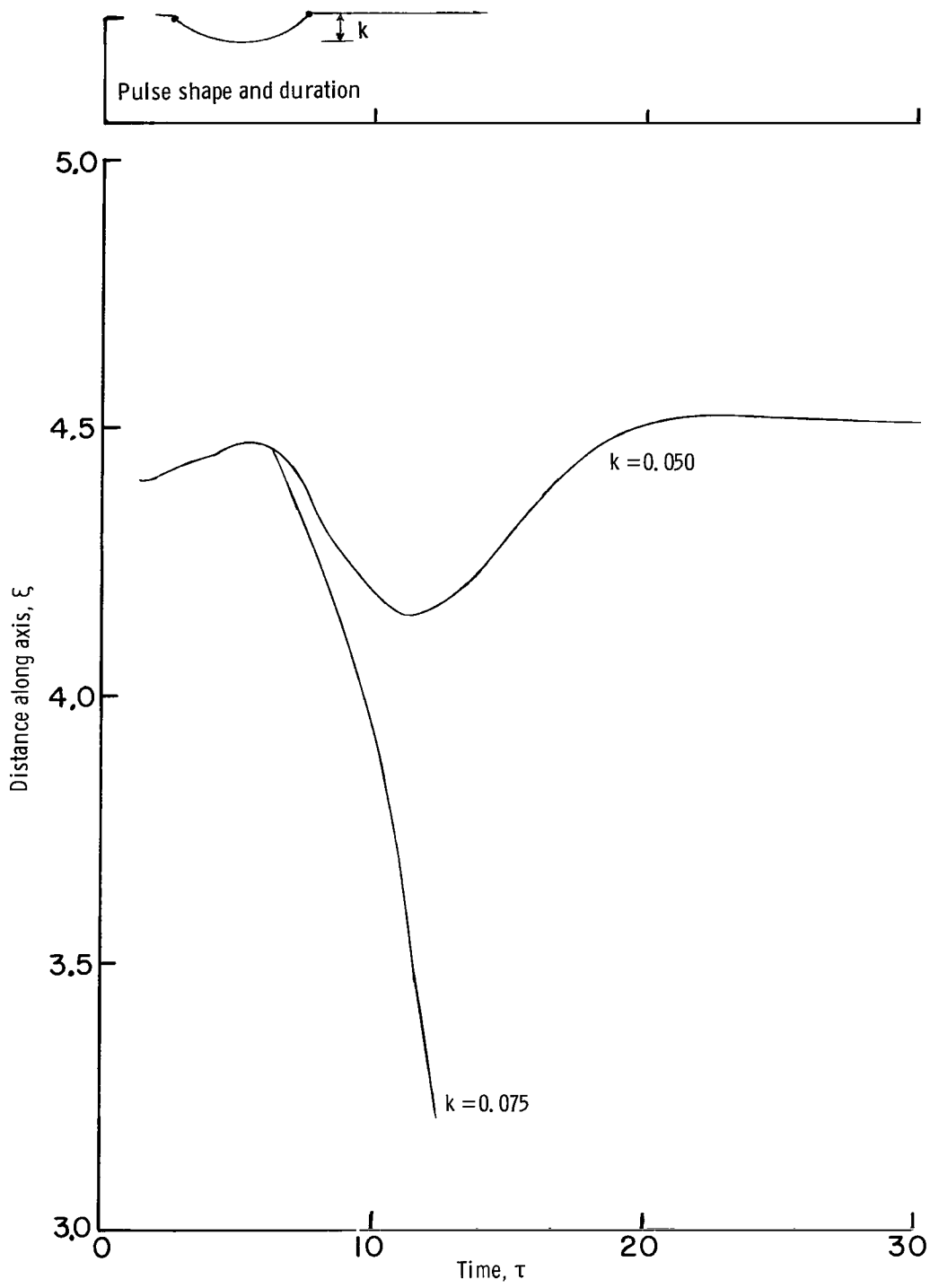

(a) Solid wall.

Figure 8.- Shock motion due to sinusoidal impulse in engine-face pressure.

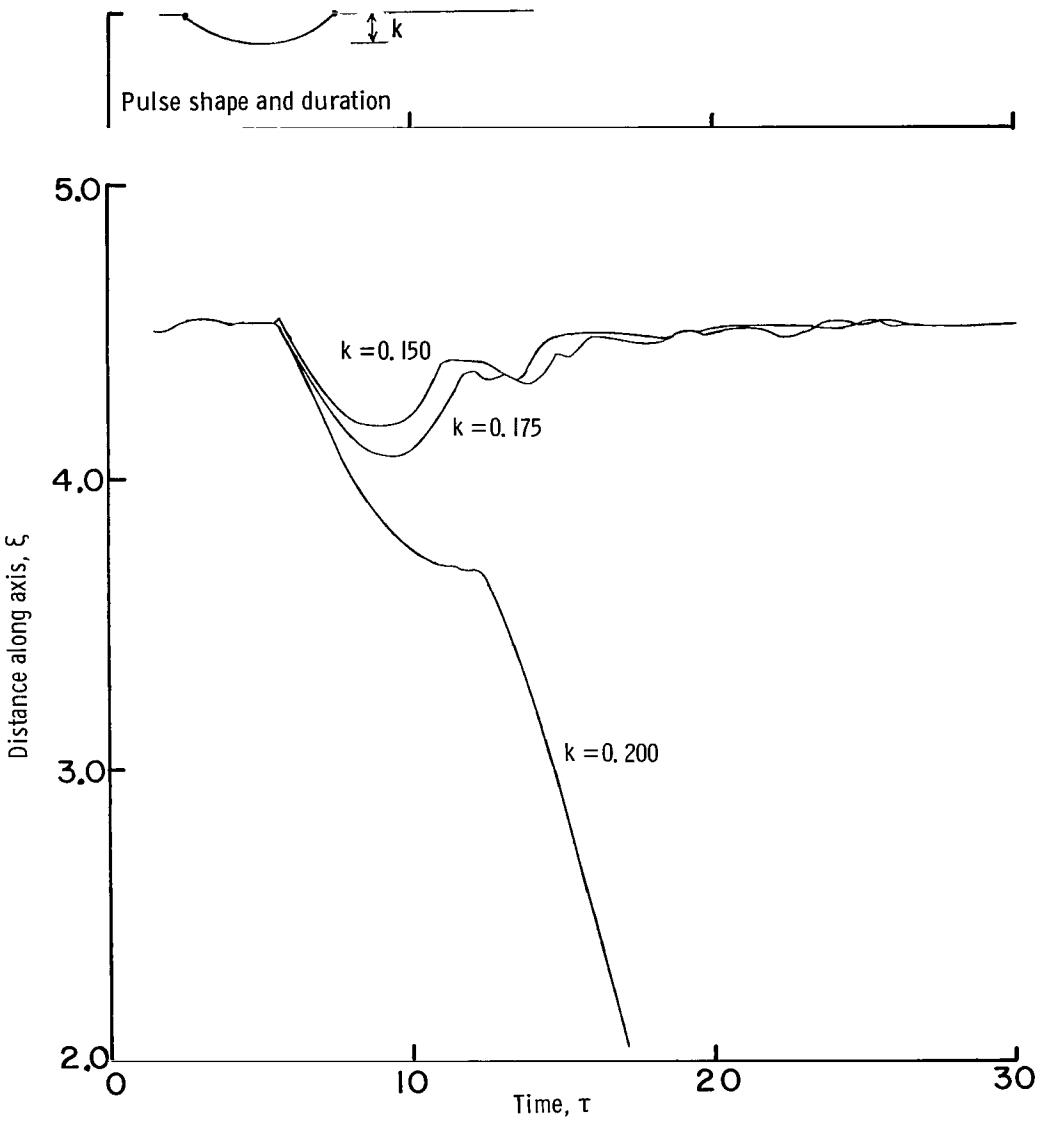

(b) 20-percent perforated wall.

Figure 8.- Continued.

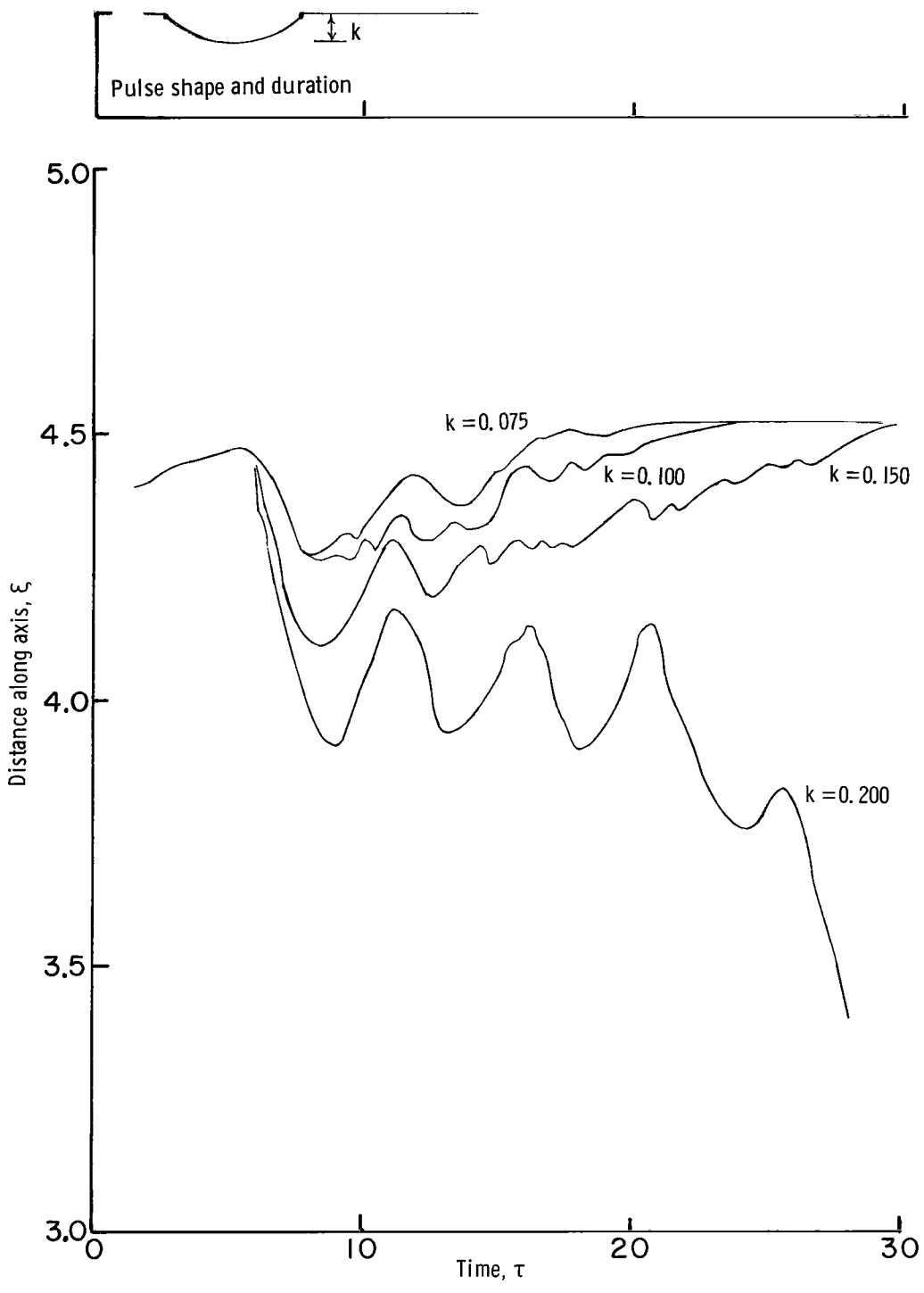

(c) 40-percent perforated wall.

Figure 8.- Concluded.

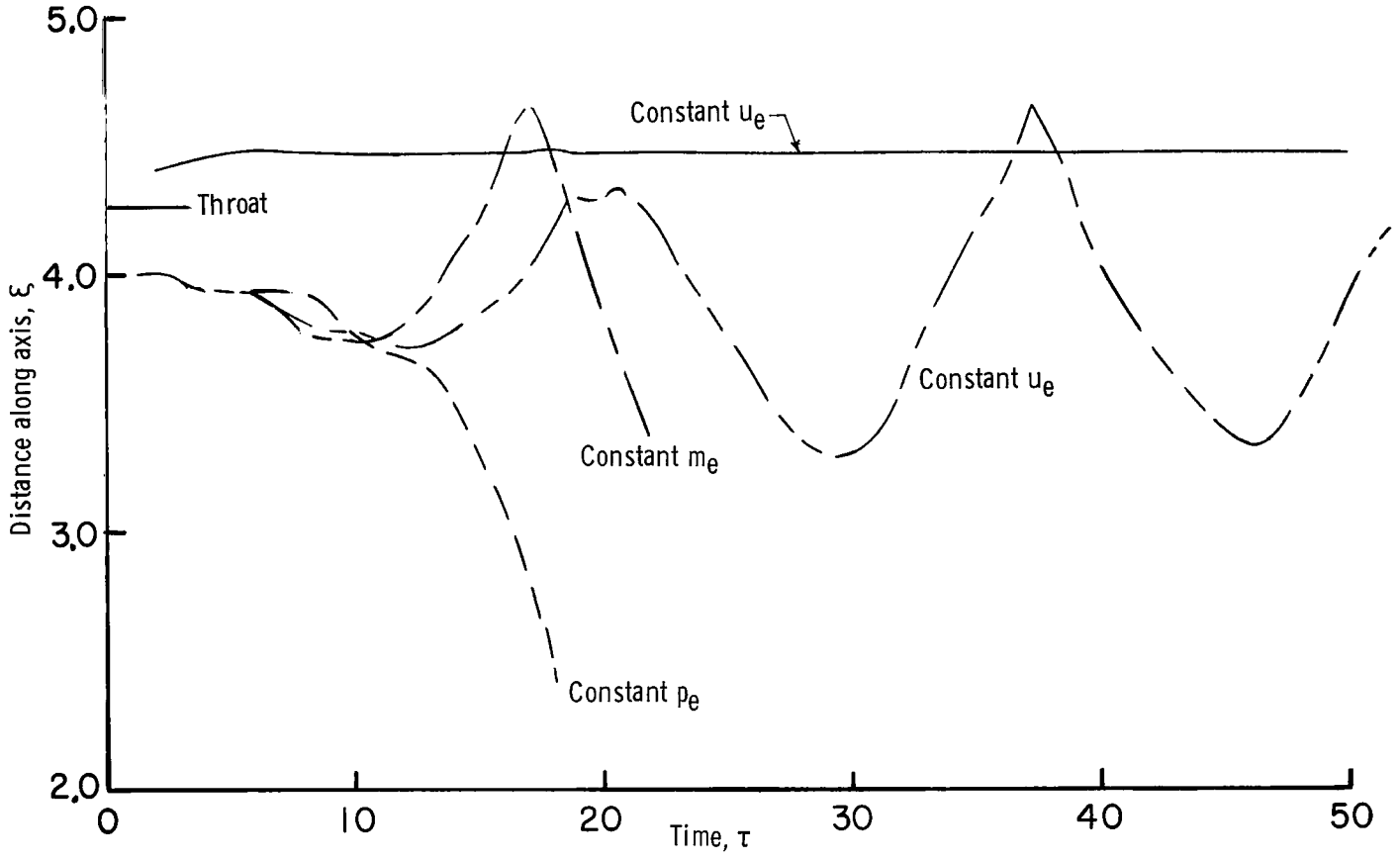

(a) Shock started at two different initial locations.

Figure 9.- Shock motion for steady-state end conditions. Distributed perforated wall.

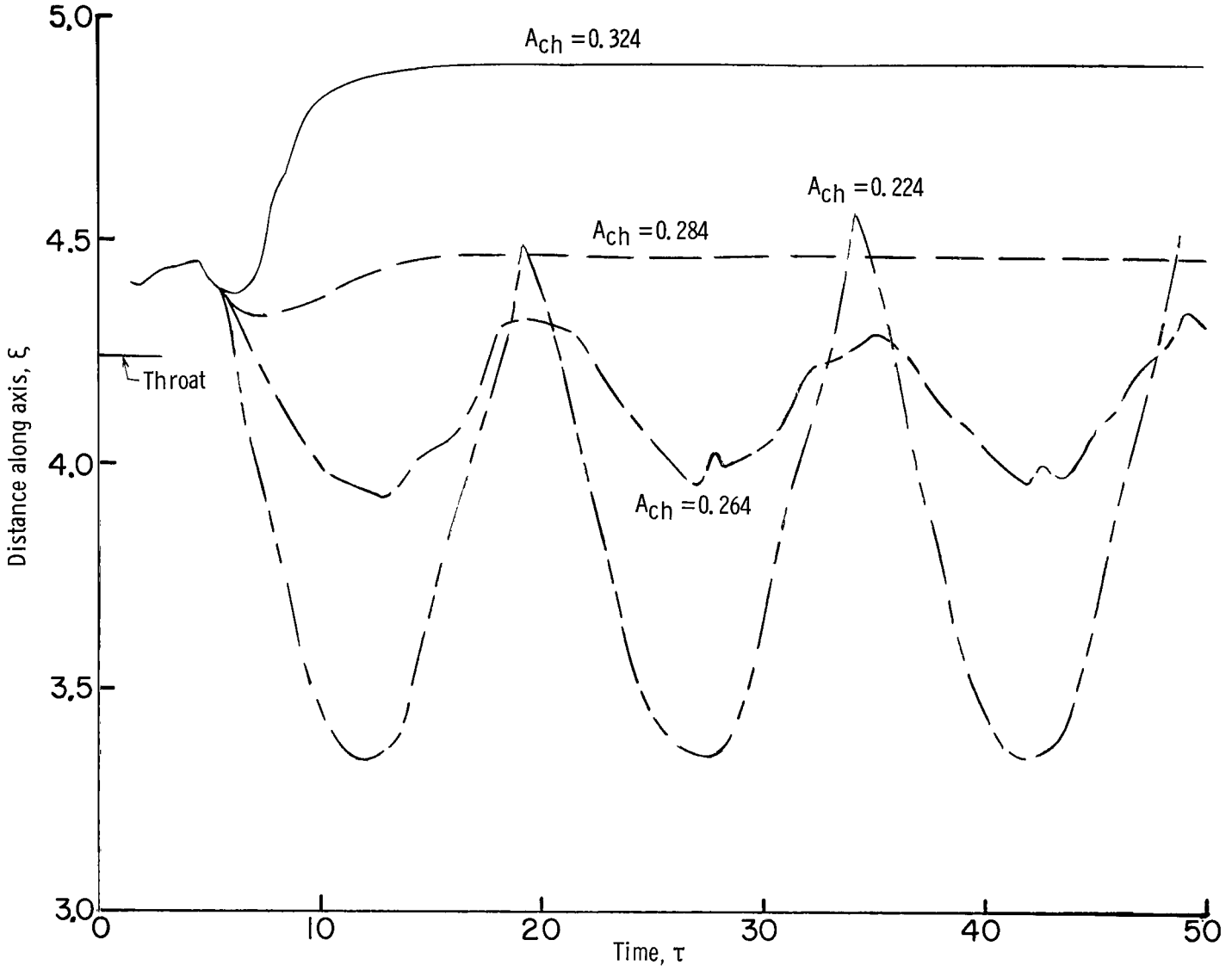

(b) Choked flow at end of inlet.

Figure 9.- Concluded.

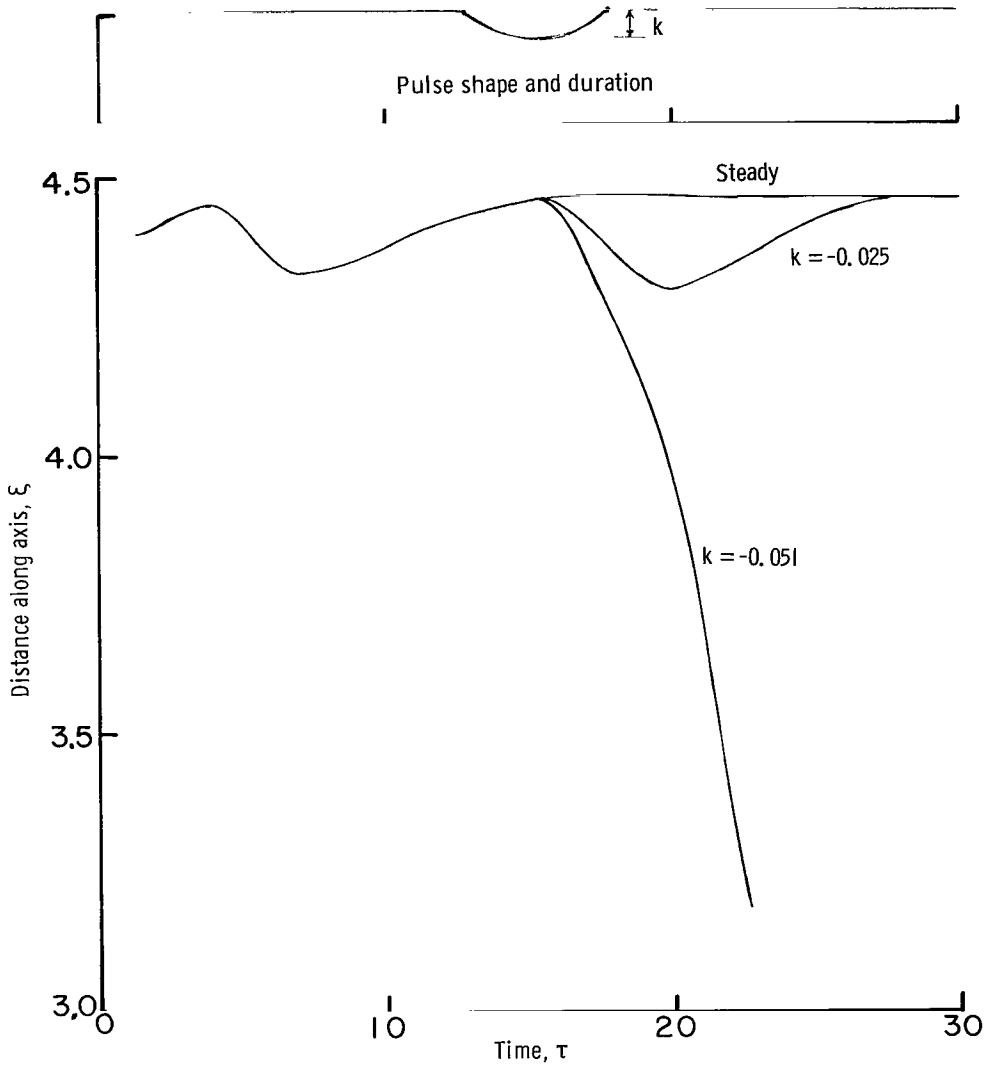

(a) Solid wall inlet.

Figure 10.- Shock motion due to sinusoidal-impulse variation of choked area at engine face. A_{ch} = 0.284.

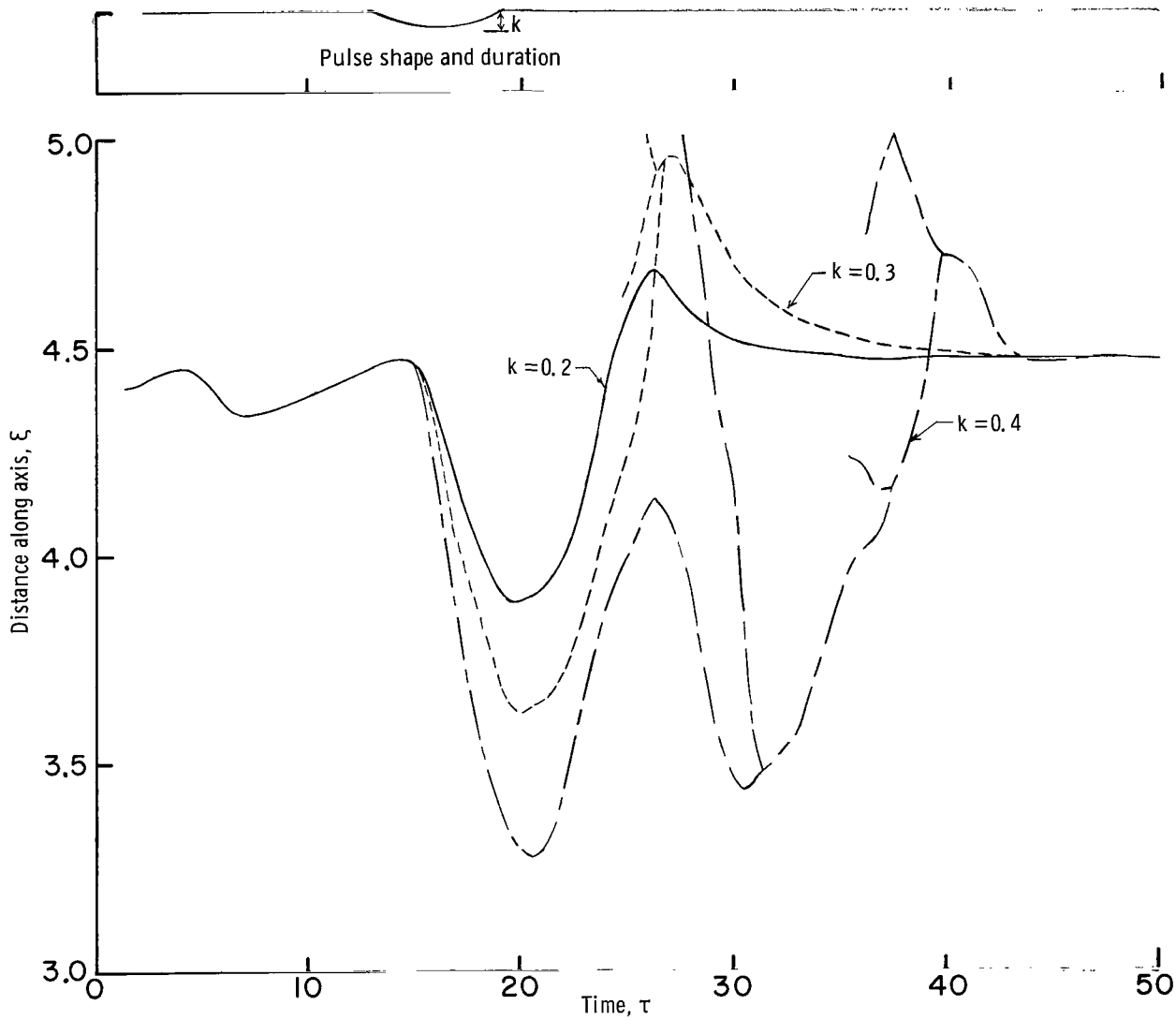

(b) Distributed perforated wall.

Figure 10.- Concluded.

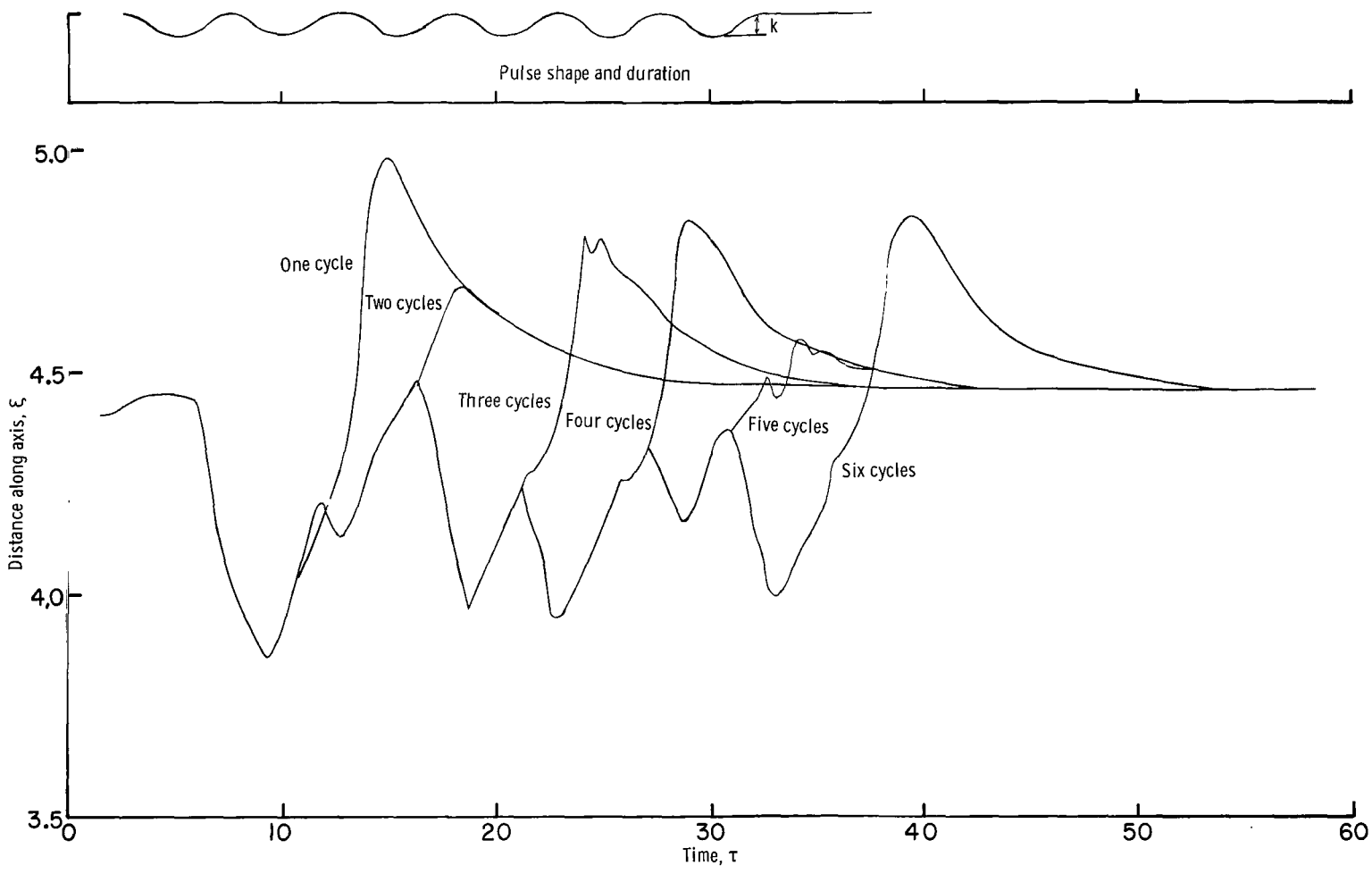

Figure 11.- Shock motion for velocity stall transients applied for periods of 1 to 6 cycles. k = -0.4; 40-percent perforated wall to station 4.2.

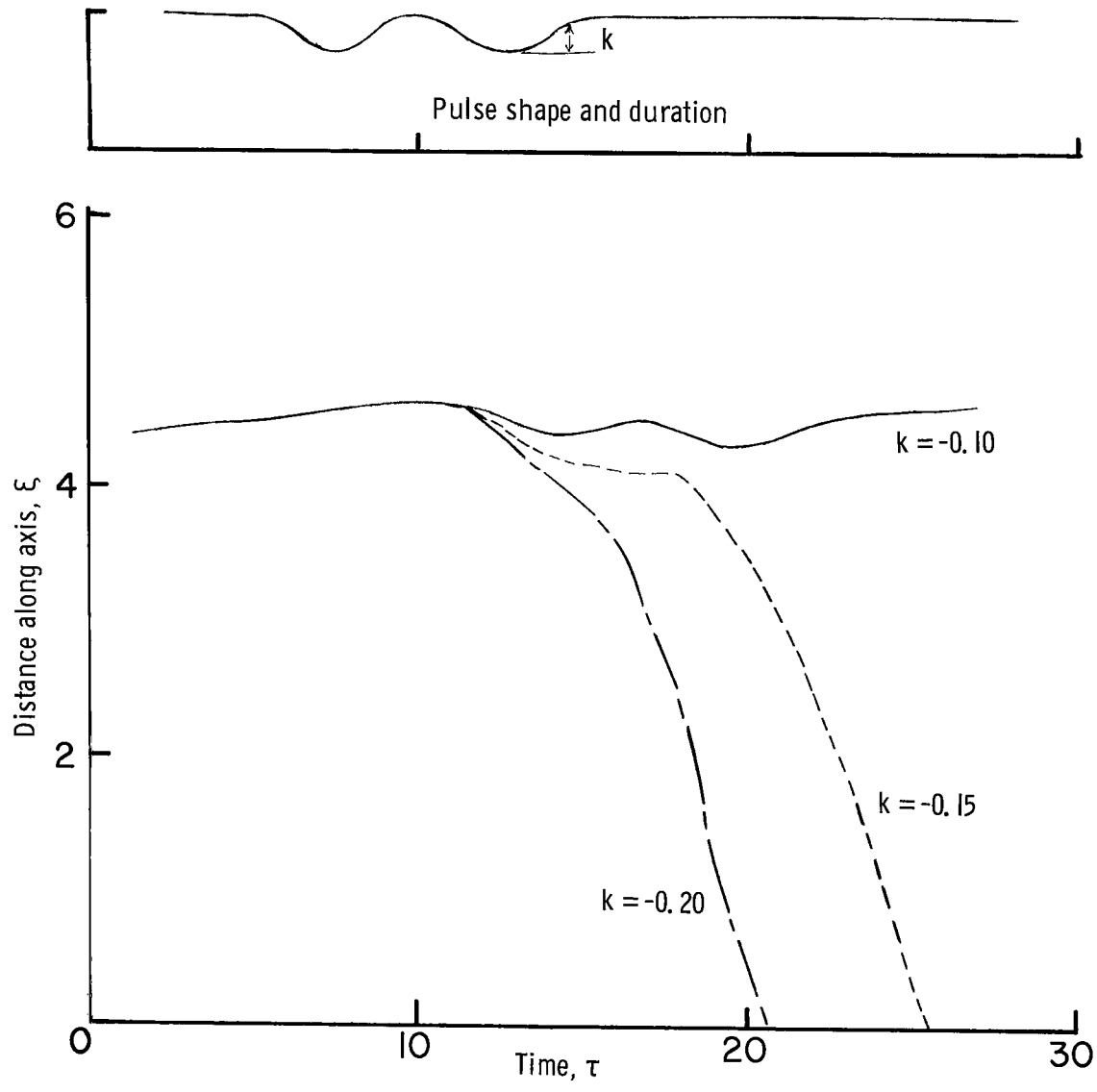

(a) Two cycles, solid wall.

Figure 12.- Shock motion due to several stall transients.

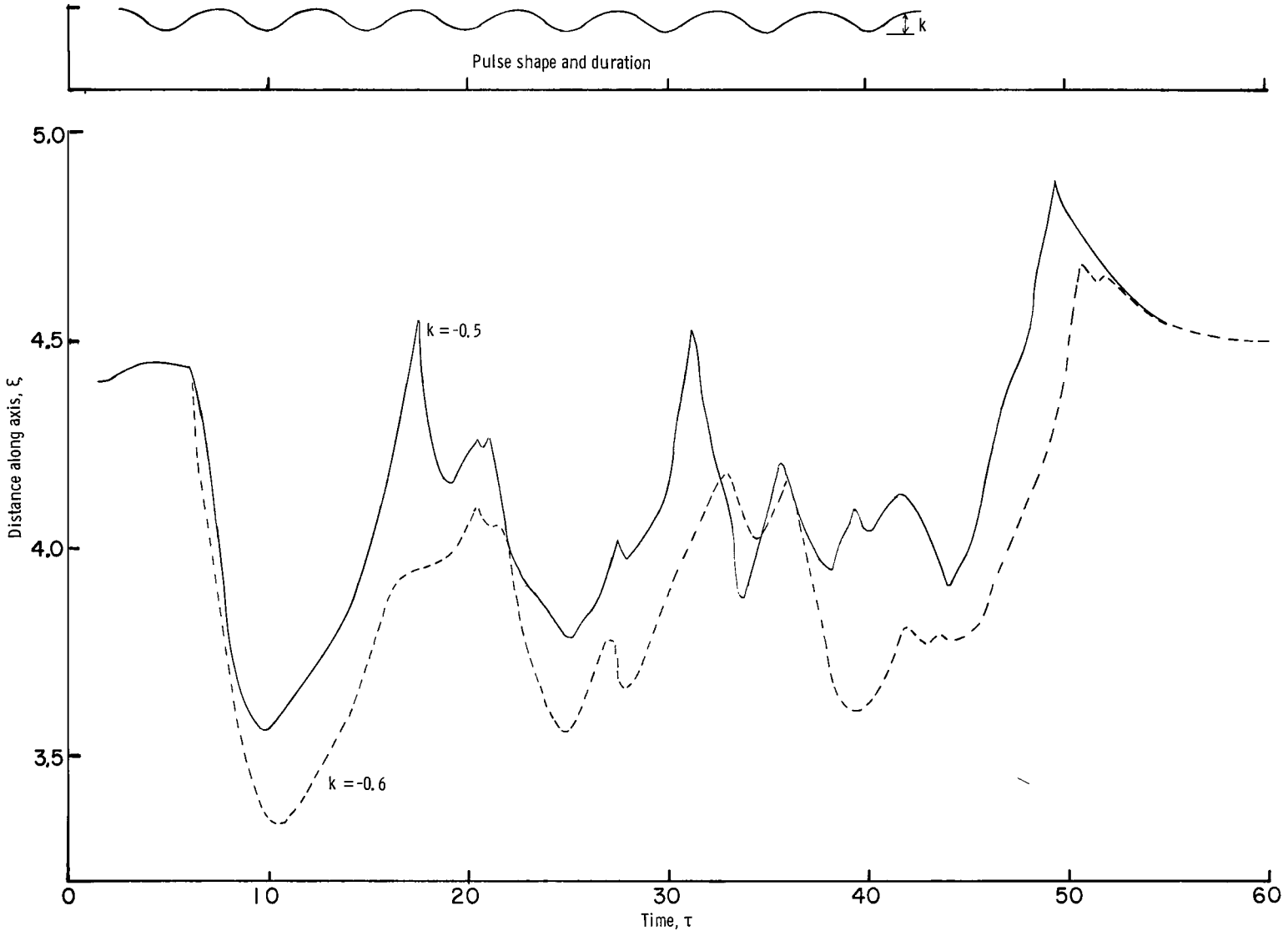

(b) Eight cycles, 40-percent perforated wall to station 4.2.

Figure 12.- Concluded.

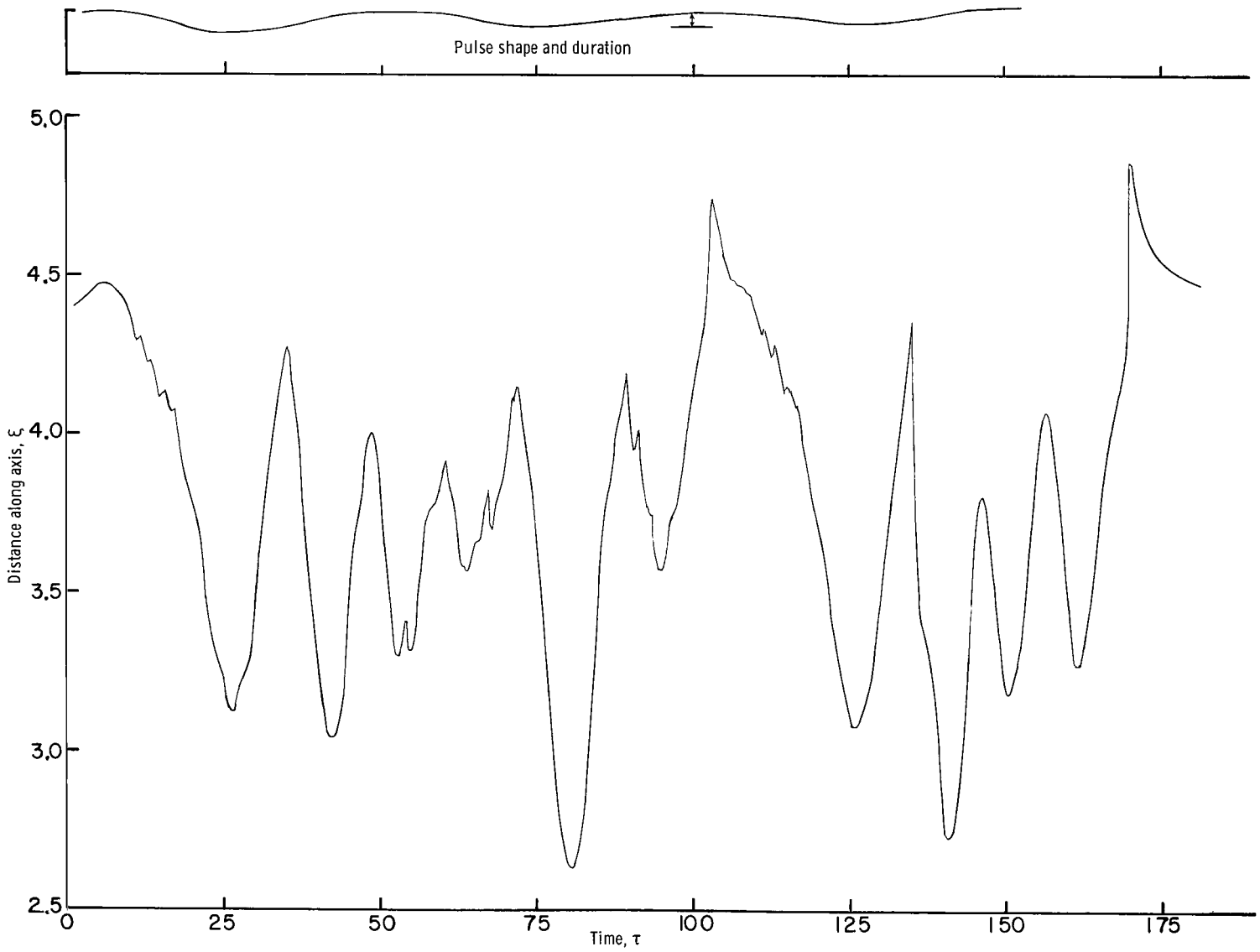

Figure 13.- Shock motion due to engine-face stall-like velocity transient. Period = 50; 40-percent perforated wall to station 4.2; k = -0.65.

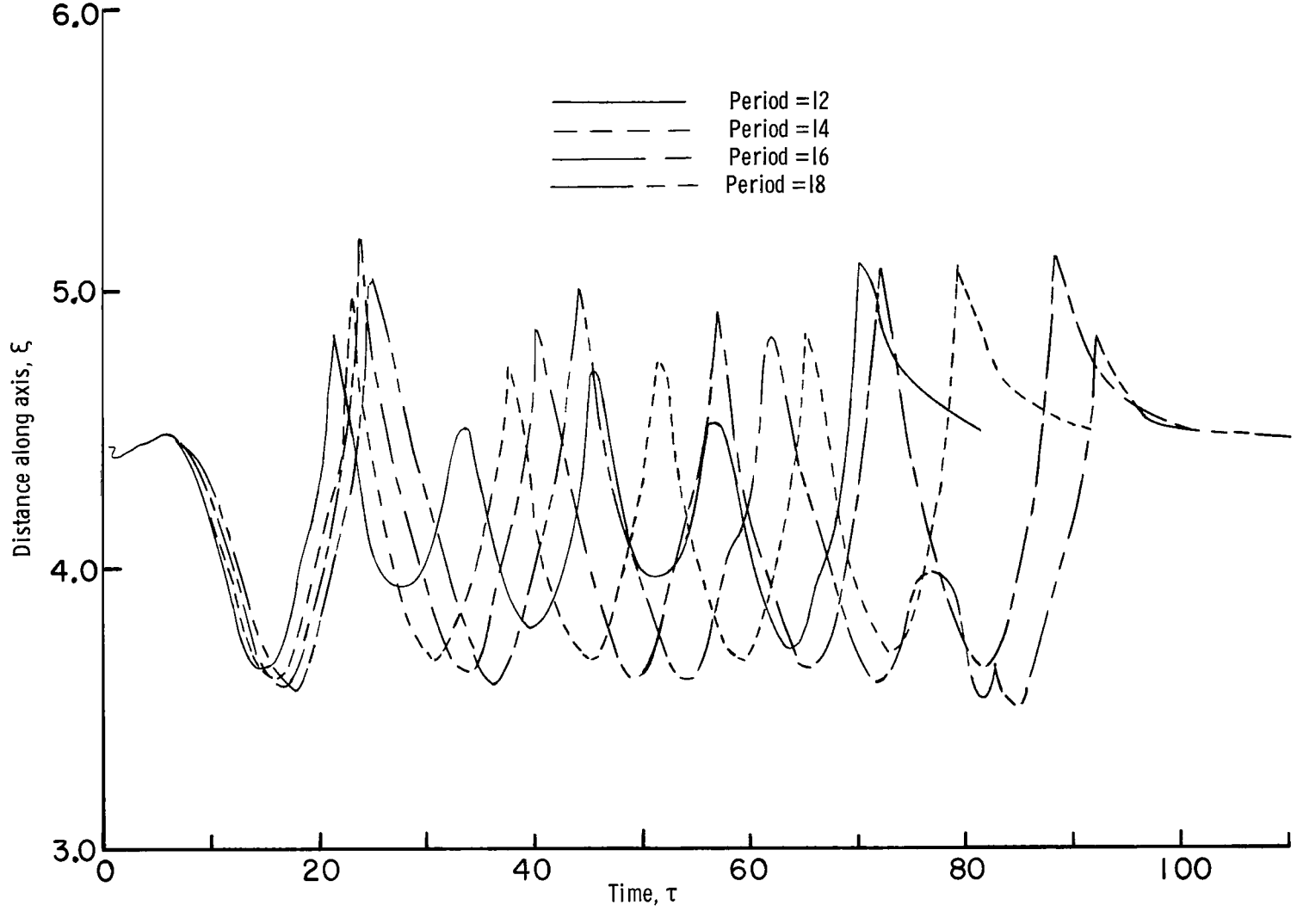

Figure 14.- Shock motion due to engine-face stall-like velocity transient for 5 cycles with periods of 12 to 18. k = -0.20.

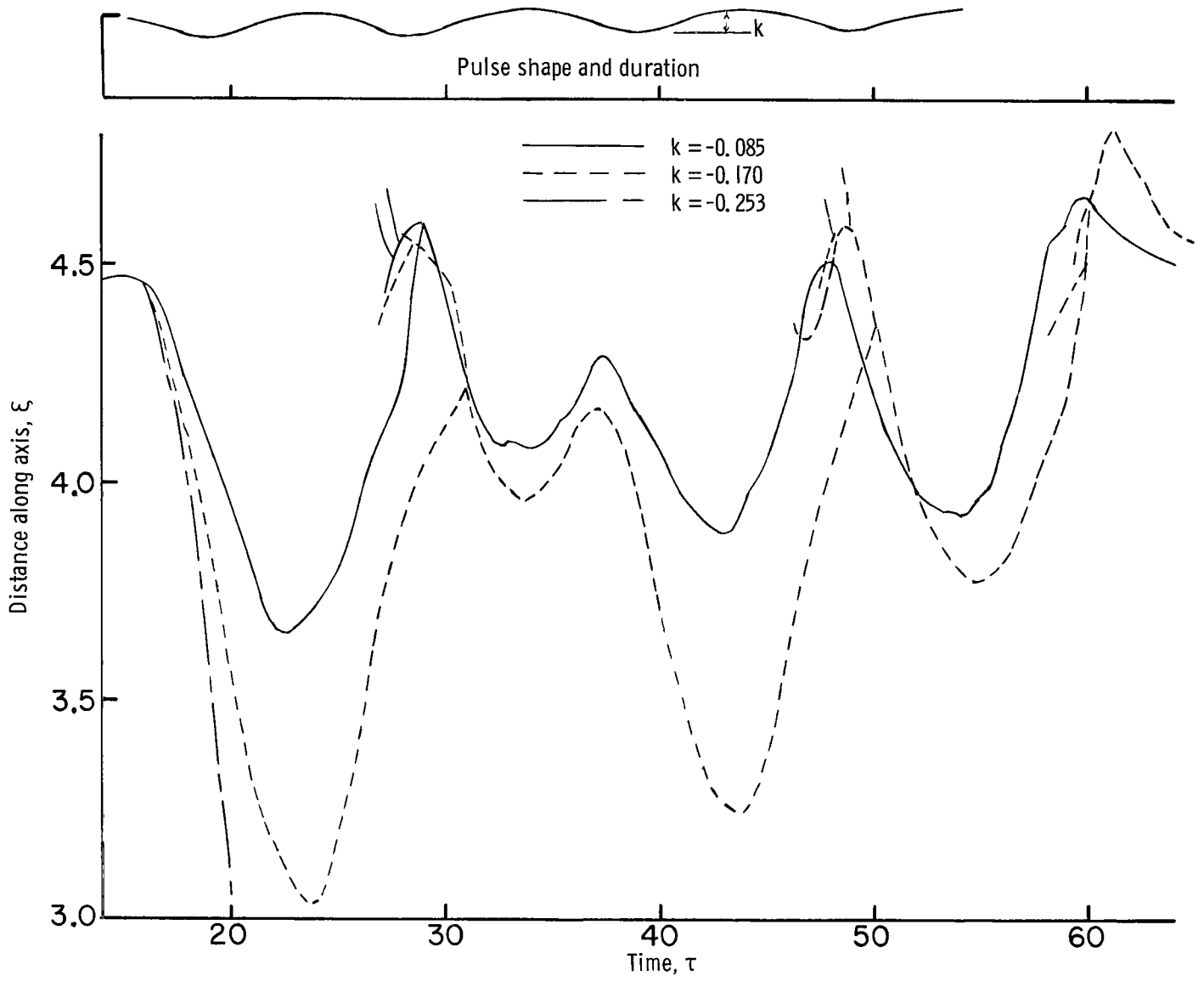

Figure 15.- Shock motion due to stall-simulation variations of the choked area at the engine face. Four cycles from τ = 14 to 54; distributed perforated wall.

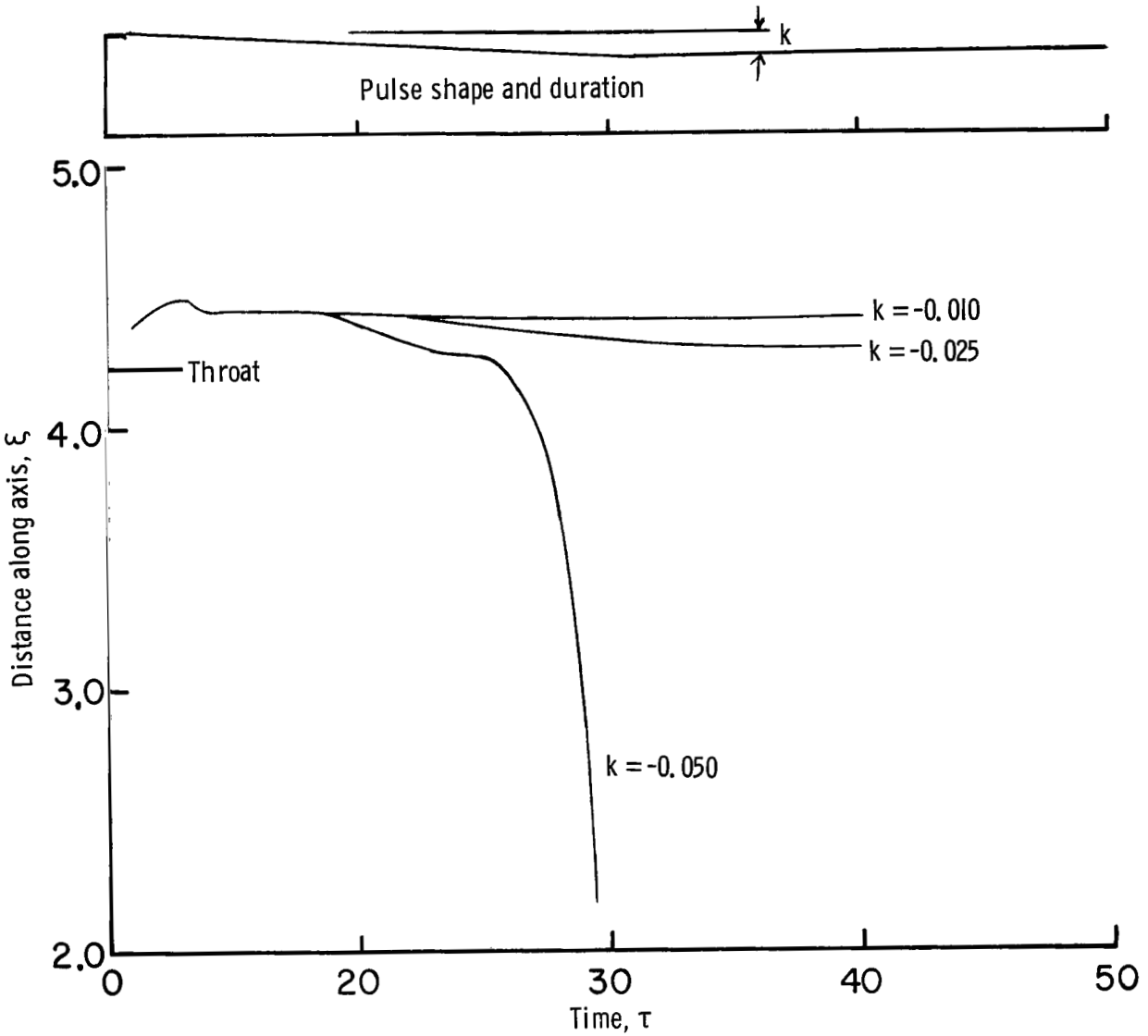

Figure 16.- Shock motion for velocity ramp transient in inlet with solid walls.

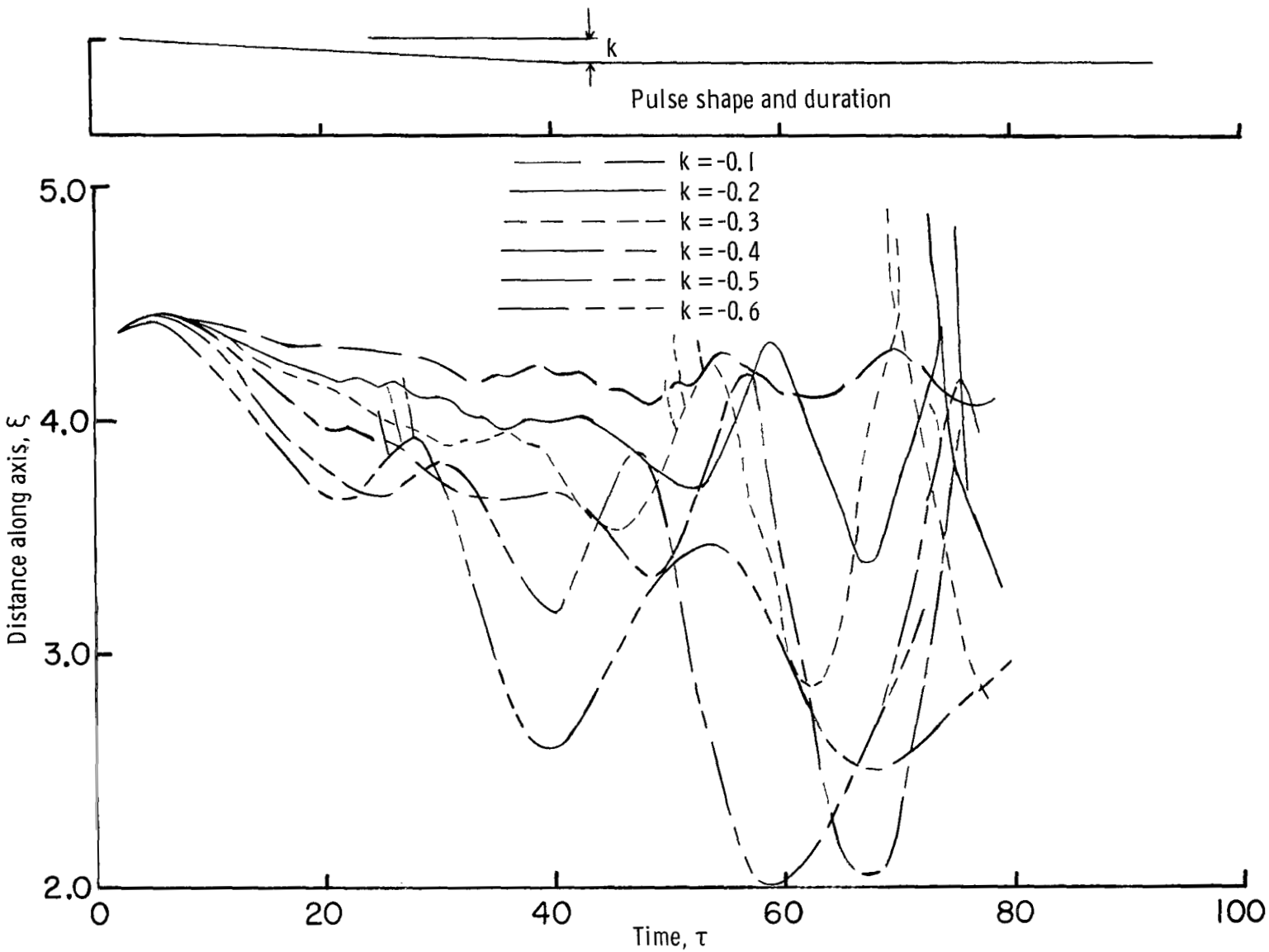

Figure 17.- Shock motion for ramp transient in engine-face velocity in an inlet with a distributed perforated wall.

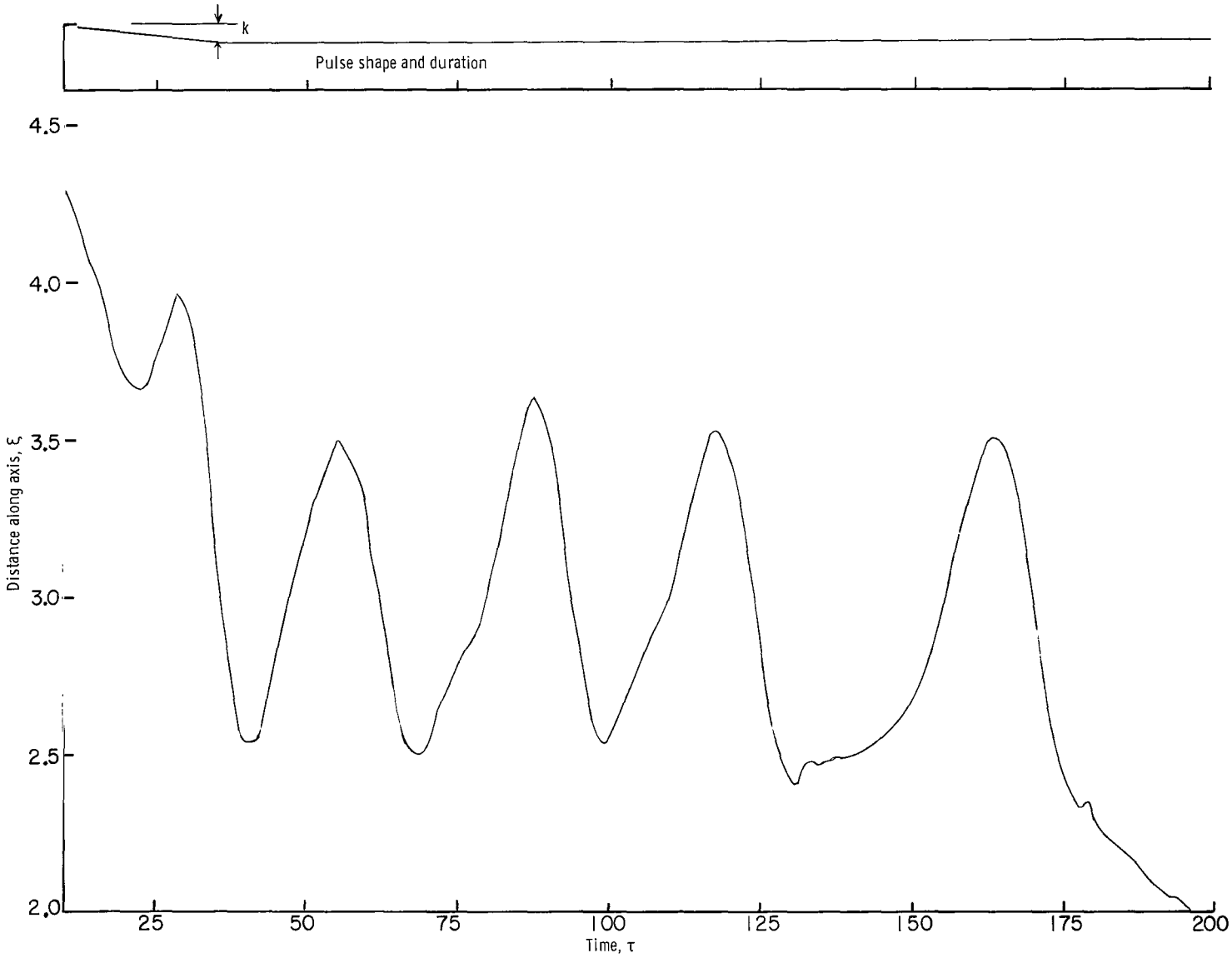

Figure 18.- Shock motion for ramp transient in engine-face velocity in an inlet with a distributed perforated wall from τ = 0 to 40. k = -0.6.

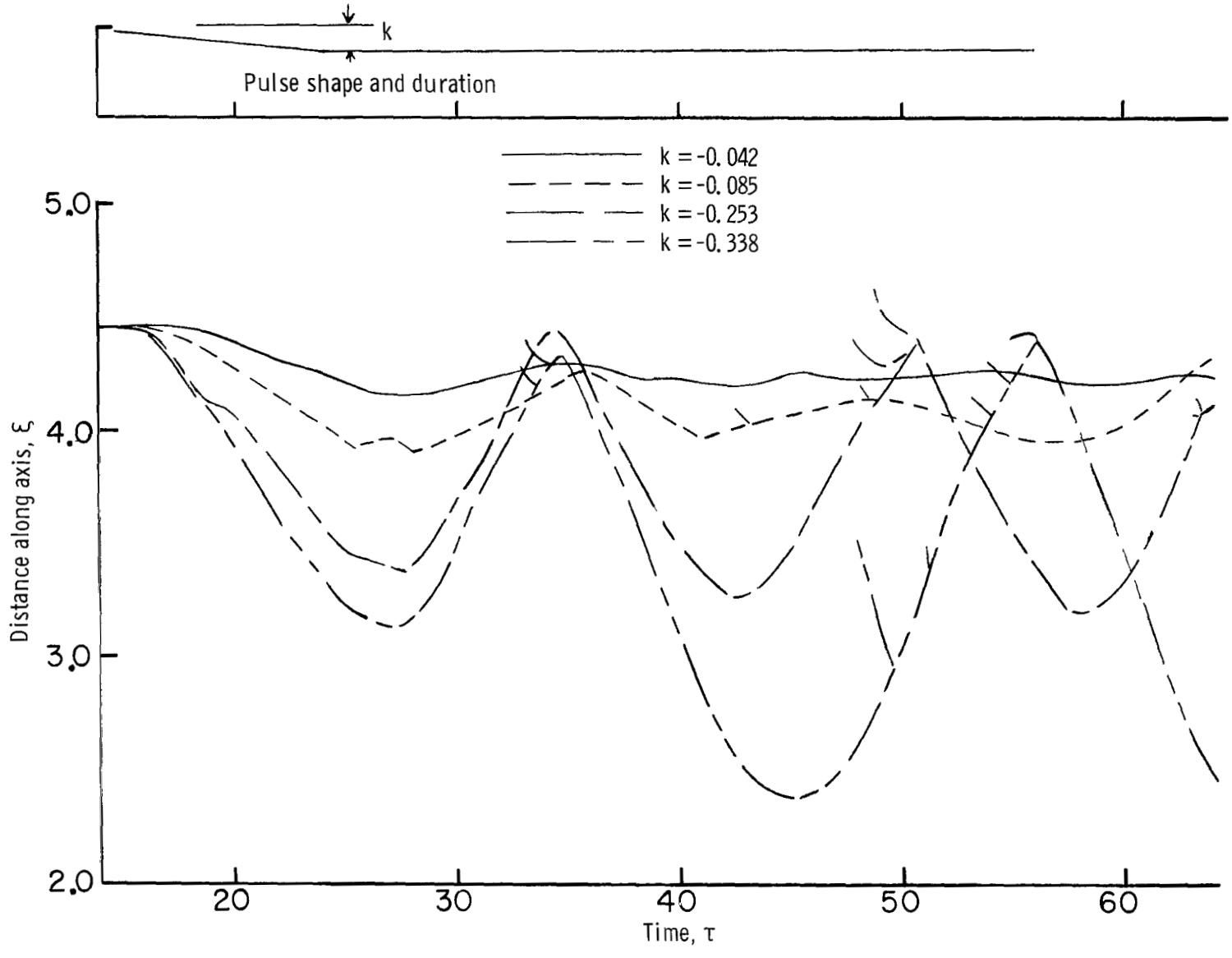

Figure 19.- Shock motion due to a ramp variation of the choked area at the engine face. Distributed perforated wall.

NATIONAL AERONAUTICS AND SPACE ADMINISTRATION
WASHINGTON, D. C. 20546

OFFICIAL BUSINESS

FIRST CLASS MAIL

POSTAGE AND FEES PAID
NATIONAL AERONAUTICS AND
SPACE ADMINISTRATION

POSTMASTER: If Undeliverable (Section 158 Postal Manual) Do Not Return

"The aeronautical and space activities of the United States shall be conducted so as to contribute . . . to the expansion of human knowledge of phenomena in the atmosphere and space. The Administration shall provide for the widest practicable and appropriate dissemination of information concerning its activities and the results thereof."

—NATIONAL AERONAUTICS AND SPACE ACT OF 1958

NASA SCIENTIFIC AND TECHNICAL PUBLICATIONS

TECHNICAL REPORTS: Scientific and technical information considered important, complete, and a lasting contribution to existing knowledge.

TECHNICAL NOTES: Information less broad in scope but nevertheless of importance as a contribution to existing knowledge.

TECHNICAL MEMORANDUMS: Information receiving limited distribution because of preliminary data, security classification, or other reasons.

CONTRACTOR REPORTS: Scientific and technical information generated under a NASA contract or grant and considered an important contribution to existing knowledge.

TECHNICAL TRANSLATIONS: Information published in a foreign language considered to merit NASA distribution in English.

SPECIAL PUBLICATIONS: Information derived from or of value to NASA activities. Publications include conference proceedings, monographs, data compilations, handbooks, sourcebooks, and special bibliographies.

TECHNOLOGY UTILIZATION PUBLICATIONS: Information on technology used by NASA that may be of particular interest in commercial and other non-aerospace applications. Publications include Tech Briefs, Technology Utilization Reports and Notes, and Technology Surveys.

Details on the availability of these publications may be obtained from:

SCIENTIFIC AND TECHNICAL INFORMATION DIVISION

NATIONAL AERONAUTICS AND SPACE ADMINISTRATION

Washington, D.C. 20546